G Protein-Coupled Receptor Kinase-2 (GRK-2) regulates exploration through neuropeptide signaling in *Caenorhabditis elegans*

Kristen Davis[1,2,3], Christo Mitchell[4,+], Olivia Podhaisky[4,+], Jihong Bai[5], David M. Raizen[1,6], Michael Ailion[4], and Irini Topalidou[4,5,*]

[1]Department of Neurology, Perelman School of Medicine, University of Pennsylvania, Philadelphia, PA, USA

[2]Center for Excellence in Environmental Toxicology (CEET), Perelman School of Medicine, University of Pennsylvania, Philadelphia, PA, USA

[3]Department of Neuroscience, Vickie and Jack Farber Institute of Neuroscience, Thomas Jefferson University, Philadelphia, PA, USA

[4]Department of Biochemistry, University of Washington, Seattle, WA, USA

[5]Fred Hutchinson Cancer Center, Seattle, WA, USA

[6]Chronobiology and Sleep Institute, Perelman School of Medicine, University of Pennsylvania, Philadelphia, PA, USA.

[+]These authors contributed equally to this work

[*]Corresponding author

Email: etopalid@fredhutch.org

Short title: GRK-2 controls exploration and movement quiescence

Abstract

Animals alter their behavior in manners that depend on environmental conditions as well as their developmental and metabolic states. For example, *C. elegans* is quiescent during larval molts or during conditions of satiety. By contrast, worms enter an exploration state when removed from food. Sensory perception influences movement quiescence (defined as a lack of body movement), as well as the expression of additional locomotor states in *C. elegans* that are associated with increased or reduced locomotion activity, such as roaming (exploration behavior) and dwelling (local search). Here we find that movement quiescence is enhanced, and exploration behavior is reduced in G protein-coupled receptor kinase *grk-2* mutant animals. *grk-2* was previously shown to act in chemosensation, locomotion, and egg-laying behaviors. Using neuron-specific rescuing experiments, we show that GRK-2 acts in multiple ciliated chemosensory neurons to control exploration behavior. *grk-2* acts in opposite ways from the cGMP-dependent protein kinase gene *egl-4* to control movement quiescence and exploration behavior. Analysis of mutants with defects in ciliated sensory neurons indicates that *grk-2* and the cilium-structure mutants act in the same pathway to regulate exploration behavior. We find that GRK-2 controls exploration behavior in an opposite manner from the neuropeptide receptor NPR-1 and the neuropeptides FLP-1 and FLP-18. Finally, we show that secretion of the FLP-1 neuropeptide is negatively regulated by GRK-2 and that overexpression of FLP-1 reduces exploration behavior. These results define neurons and molecular pathways that modulate movement quiescence and exploration behavior.

Author summary

Many modulatory neurotransmitters affect behavior by binding to G protein-coupled receptors (GPCRs) and initiating signals that modify neuronal activity. GPCRs are regulated by G protein-coupled receptor kinases (GRKs). GRKs phosphorylate and promote the inactivation of GPCRs. Here we identify GRK-2 as a regulator of distinct locomotor states in *C. elegans*. We find that GRK-2 acts in olfactory sensory neurons to promote exploration and suppress movement quiescence. Additionally, we show that GRK-2 acts in opposition to a neuropeptide signaling pathway that acts in interneurons. Thus, this study demonstrates critical roles for GRK-2 in regulating neuromodulatory signaling and locomotor behavior.

Introduction

Animals modify their behaviors in response to changes in their environment or metabolic state. Sensory and neuromodulatory signals play a major role in adapting behavior to environmental or metabolic changes [1-6]. For example, animals experience periods of quiescence and arousal that depend on sensory and neuromodulatory cues [3,5,7-9]. Arousal is a state of increased responsiveness that can be associated with fear or starvation, whereas quiescence is characterized by decreased responsiveness and is associated with sleep and satiety. Even though sensory and neuromodulatory signals are recognized as major modulators of behavior, the precise mechanisms that mediate behavioral strategies under different inputs remain largely unknown. Here we describe how a locomotor behavior in the nematode *Caenorhabditis elegans* is altered through the action of the G protein-coupled receptor kinase-2 (GRK-2) in sensory neurons and neuromodulator signaling in interneurons.

Several examples of movement quiescence in response to changes in the external environment or the internal metabolic state of the animal have been reported in *C. elegans. C. elegans* enters an exploration state when it is removed from food [10,11] and becomes quiescent during molting or under conditions of prolonged starvation, satiety, or cellular stress [3,12-17]. Sensory perception affects quiescence, as well as additional locomotor states in *C. elegans* that are characterized by increased or reduced locomotion activity, such as roaming/exploration and dwelling [2]. The animal covers a large area during roaming (exploring), while it restricts its activity to a small region during the dwelling state. The mechanism by which sensory perception modulates this locomotor strategy is unknown.

Quiescence, roaming, and dwelling are controlled by the function of the cGMP-dependent protein kinase (PKG) gene *egl-4* in sensory neurons. *egl-4* loss-of-function mutant animals have chemosensory defects [18] and attenuated sensory adaptation [19]. EGL-4 is a regulator of lethargus quiescence, a sleep-like behavior that takes place during molts [3], and of a satiety-induced sleep-like behavior [12]. EGL-4 also defines the time the animals spend

84 roaming and dwelling since *egl-4* loss of function mutant animals show increased exploration
85 [2,20]. Here, we describe a role for GRK-2 in the sensory neurons of *C. elegans* to regulate
86 movement quiescence and exploration in an opposite manner to EGL-4.

87 GRKs play key roles in attenuating the strength of neuromodulatory pathways by
88 phosphorylating G protein-coupled receptors (GPCRs) and promoting the inactivation of GPCR
89 signaling [21]. Vertebrates have seven GRKs that are classified into three subfamilies: the visual
90 GRKs (GRK1/7), the GRK2/3 subfamily, and the GRK4/5/6 subfamily [22]. *C. elegans,* which
91 lacks a visual system, has GRK-1 and GRK-2, which are orthologs of the mammalian GRK4/5/6
92 and GRK2/3 families, respectively [23,24]. *grk-2* is expressed broadly in the nervous system
93 and has a broad impact on animal physiology including chemosensation [23], gustatory
94 plasticity [25], egg-laying [26], crawling [27], swimming [27,28], and oxidative and heat stress
95 responses [29,30]. Elimination of *grk-2* function renders animals unable to respond to a wide
96 range of chemical stimuli, suggesting that GRK-2 plays a positive role in chemosensation [23].
97 Similarly, *grk-2* mutant animals show reduced crawling rates and are unable to swim, again
98 suggesting that GRK-2 plays a positive role in regulating crawling and swimming [27,28]. GRK-2
99 was proposed to promote crawling and swimming by negatively regulating the D2-like dopamine
100 receptor DOP-3 [27,28]. GRK-2 regulates chemosensation by acting in sensory neurons [23],
101 but it controls crawling and swimming by acting in premotor interneurons [27,28], suggesting
102 that GRK-2 acts in different neurons to modulate distinct behavioral outcomes.

103 Besides sensory perception, neuromodulation has also been shown to play a critical role
104 in defining arousal and quiescence as well as roaming and dwelling in *C. elegans*. For example,
105 mutants lacking the neuropeptide receptor NPR-1 have been used as a model for studying
106 arousal since both lethargus and movement quiescence are reduced in *npr-1* mutants [8,31-33].
107 Specifically, increased RMG interneuron activity in *npr-1* mutant animals during lethargus
108 induces secretion of the neuropeptide pigment dispersing factor PDF-1, resulting in increased
109 animal motility and reduced quiescence [31]. PDF-1 also positively regulates roaming, whereas

110 serotonin plays an opposite role by increasing dwelling [4]. Here we find that GRK-2 regulates
111 exploration in an opposite manner to NPR-1 and the neuropeptides FLP-1 and FLP-18. We also
112 show that GRK-2 acts in different pathways than PDF and serotonergic signaling. Finally, we
113 demonstrate that secretion of FLP-1, a neuropeptide that regulates locomotion [34-37], depends
114 on GRK-2 and that overexpression of *flp-1* inhibits exploration behavior.
115

Results

GRK-2 regulates exploration and dispersal in a DOP-3- independent way

Our previous work suggested that GRK-2 positively regulates crawling and swimming by negatively regulating the D2-like dopamine receptor DOP-3 [27,28]. *grk-2(gk268)* null mutant animals exhibit slow crawling and impaired swimming, and mutations in *dop-3* suppress both these phenotypes. *grk-2* mutant animals also have a decreased exploration behavior: they restrict their movements to a limited region of the bacterial lawn, whereas wild-type animals explore the entire lawn [27]. We used simple radial locomotion and exploration assays ([4,38]; see also Methods) to quantify this phenotype by observing the radial distance that individual animals traveled over 1 h (Fig 1A) or the tracks that individual animals left on a lawn of *E. coli* over an 18-20 hr period (Fig 1D). We found that *grk-2(gk268)* mutant animals disperse and explore less compared to wild-type (Fig 1B and 1E). This phenotype is independent of sex since *grk-2* males also explore less than wild type males (Fig 1F). To examine whether the *grk-2* dispersal defect depends on the presence of food we performed the dispersal assay on plates without *E. coli.* We found that *grk-2(gk268)* mutant animals disperse less compared to wild type even in the absence of the bacteria lawn (Fig 1C), suggesting that the dispersal defect of *grk-2* mutant is independent of the presence or absence of food.

Although the *dop-3(vs106)* mutation suppresses the slow locomotion and swimming defects of *grk-2(gk268)* mutant animals [27,28], it did not significantly alter the dispersal or exploration behavior of *grk-2(gk268)* (Fig 1B,C and E), suggesting that GRK-2 controls the exploration behavior independently of DOP-3, and that the mechanism by which GRK-2 controls exploration is different than its role in regulating crawling and swimming.

GRK-2 acts in a different pathway than serotonergic or PDF signaling to regulate exploration

Worm exploration behavior is regulated by serotonergic and PDF signaling: serotonin

142 inhibits exploration through the MOD-1 serotonin-gated chloride channel, while PDF-1 promotes
143 exploration through the Gαs-coupled PDF receptor PDFR-1 [4]. To examine whether GRK-2
144 acts in the PDF-1 pathway to control exploration we compared animals that were mutant for
145 both *grk-2* and *pdfr-1* to single mutants. We found that *pdfr-1(ok3425)* mutant animals display
146 decreased exploration, as previously reported [4] and that the phenotype of the double mutant
147 *grk-2(gk268); pdfr-1(ok3425)* is stronger than the phenotype of the single mutants (Fig S1A),
148 suggesting that GRK-2 and PDFR-1 act in different pathways to control exploration. Similarly, to
149 examine whether GRK-2 acts in the serotonin pathway to control exploration, we built double
150 mutants between *grk-2* and *tph-1* mutants (*tph-1* encodes the rate-limiting enzyme for serotonin
151 synthesis). We verified that *tph-1(mg280)* mutant animals display increased exploration [4] and
152 further showed that *grk-2(gk268); tph-1(mg280)* double mutant animals have an intermediate
153 phenotype between that of either *grk-2* or *tph-1* single mutants (Fig S1B), suggesting that *grk-2*
154 and *tph-1* act in separate pathways to control exploration. Our results imply that GRK-2 acts in a
155 different pathway than serotonergic or PDF signaling to regulate exploration.
156
157 **GRK-2 functions in the ciliated neurons to control exploration**
158 GRK-2 is expressed broadly in the nervous system [23] and acts in premotor
159 interneurons to control crawling and swimming [27,28]. To determine where GRK-2 acts to
160 control exploration, we expressed the *grk-2* cDNA under the control of neuron-specific
161 promoters. Expression of *grk-2* cDNA under the pan-neuronal promoter (*rab-3p*) fully
162 rescued the *grk-2(gk268)* mutant exploration defect but expression in ventral cord acetylcholine
163 motor neurons alone (using the *acr-2* promoter) or in command interneurons alone (using the
164 *nmr-1* promoter) did not rescue this defect (Fig 2A). Expression of *grk-2* cDNA in the same set
165 of command interneurons rescued the crawling defects of *grk-2* mutant animals (Fig S2),
166 supporting the notion that the role of GRK-2 in exploration is different from its role in crawling.
167 *grk-2* mutants fail to respond to a wide range of chemical stimuli, suggesting that GRK-2

168 is a positive regulator of chemosensation [23]. To test the hypothesis that the exploration defect
169 in *grk-2(gk268)* mutant animals is explained by its role in chemosensation, we expressed the
170 *grk-2* cDNA under the ciliated sensory neuron promoters *xbx-1p* and *osm-6p*. Expression of *grk-*
171 *2* cDNA in ciliated sensory neurons fully rescued the exploration defect of *grk-2* mutant animals
172 both in the presence and absence of food (Fig 2B,C). Our result that transgenic expression of
173 *grk-2* under *rab-3, xbx-1*, or *osm-6* heterologous promoters fully rescued the *grk-2* exploration
174 defect (Fig 2A-C) suggests that the precise level of GRK-2 is not critical to its function.
175 To further narrow down the site of action of GRK-2 in exploration we expressed the *grk-*
176 *2* cDNA under the control of the *odr-3* promoter (*odr-3p*), which promotes expression in olfactory
177 and nociceptive neurons: AWA, AWB, AWC, ASH, and ADF [39]. Expression of *grk-2* under the
178 *odr-3* promoter partially rescued the exploration defect of *grk-2* mutant animals, suggesting that
179 *grk-2* acts in multiple ciliated neurons to regulate exploration (Fig 2D). An operon GFP was
180 included in the expression construct downstream of the 3'UTR allowing confirmation of
181 expression (see Methods). To confirm that *grk-2* is expressed in *odr-3*- expressing neurons, we
182 expressed the cDNA encoding GRK-2 protein fused to tagRFP (*grk-2*::tagRFP) under the *grk-2*
183 promoter as well as mNeon::NLS driven by the *odr-3* promoter (*odr-3p*::mNeon::NLS). We
184 confirmed that *grk-2* is indeed expressed in *odr-3*-expressing neurons (shown with arrows in Fig
185 2G).
186 To dissect further the subset of chemosensory neurons where GRK-2 acts to control
187 exploration we expressed the *grk-2* cDNA under the control of the *sra-6* promoter, which is
188 primarily expressed in the ASH and ASI chemosensory neurons (*sra-6p*; [40]). Expression of
189 *grk-2* under the *sra-6* promoter partially rescued the *grk*-2 exploration defect, suggesting that a
190 part of GRK-2's role in exploration is due to its action in the ASH or ASI neurons (Fig 2E).
191 Similarly, *grk-2* expression in the AWA, AWB, or AWC neurons (*odr-10p*: expression in AWA
192 [41]; *str-1p*: expression in AWB [42]; *str-2p*: expression in AWC-ON [43]) only slightly rescued
193 the *grk-2* exploration defect (Fig 2F). Even *grk-2* expression under the combined control of the

194 *odr-1, str-1,* and *str-2* promoters only partially rescued the *grk-2* exploration defect (Fig 2E),
195 again suggesting that *grk-2* acts in more than a single type of ciliated neurons to control
196 exploration. To address the possibility that expression of *grk-2* in any ciliated sensory neuron
197 might rescue the exploration defect of *grk-2* mutant animals, we expressed *grk-2* under the *gcy-*
198 *8* promoter, which is solely expressed in the AFD thermosensory neurons (*gcy-8p;* [44]).
199 Expression of *grk-2* under the *gcy-8* promoter failed to rescue the *grk-2* exploration defect (Fig
200 2H). Similarly, expression of *grk-2* under the dopaminergic neuron promoter *dat-1* [45] failed to
201 rescue the *grk-2* exploration defect (*dat-1p*; Fig 2I).
202 To examine whether GRK-2 plays a developmental role in modulating exploration we
203 placed *grk-2* cDNA under the control of a heat shock-inducible promoter and introduced it in *grk-*
204 *2* mutant animals. Heat shock in adult animals partially but significantly restored the exploration
205 behavior of *grk-2* (Fig 2J). These results together suggest that GRK-2 has a functional role in
206 mature ciliated sensory neurons to regulate exploration.
207
208 **Mutants in cilia-related genes have exploration defects similar to *grk-2***
209 Mutants with defects in sensory perception exhibit exploration defects on food like the
210 ones described here for *grk-2* [2]. Specifically, mutants with cilium-structure defects (such as
211 *che-2*) restrict their movements to a limited region of the bacterial lawn, while sensory signal
212 transduction mutants like *tax-2* and *tax-4* have a weaker defect than cilium-structure mutants
213 [2]. *grk-2* mutant animals are not defective in their ability to take up a fluorescent dye like the
214 cilium-structure mutants (Dye-filling assay; [23]), an assay indicative of the structural integrity of
215 the sensory cilia. To confirm that cilium structure mutants have exploration defects similar to
216 *grk-2*, we performed the exploration assay on *che-2(e1033)* and *daf-10(e1387)* mutant animals
217 in the presence or absence of food. We found that *che-2(e1033)* and *daf-10(e1387)* mutant
218 animals are exploration defective identical to *grk-2(gk268*) (Fig 3A-C). Additionally, the *che-*
219 *2(e1033)* and *daf-10(e1387)* mutations do not enhance the phenotype of *grk-2* mutant (Fig 3A-

220 C). The lack of an obvious enhancement is not due to a floor effect since *grk-2; pdfr-1* double
221 mutant animals have stronger exploration phenotype than the single mutants (Fig S1A). These
222 findings suggest that *che-2, daf-10*, and *grk-2* act in the same pathway to regulate exploration
223 (Fig 3A-C).

224 To further investigate which kinds of sensory perception affect exploration, we used the
225 exploration assay to test mutants with different sensory defects. Most chemosensory and
226 osmosensory- defective mutants that possess defective cilia based on their Dye filling
227 phenotype [46] had defects in exploration (Fig 3D). Specifically, mutants with strong cilium-
228 structure defects (shown in blue in Fig 3D) had strong exploration defects and most mutants
229 with weak cilium defects (shown in green in Fig 3D) had weaker exploration defects. Other
230 chemosensory, osmosensory, and thermosensory defective mutants (*odr-1, odr-3, odr-8, odr-*
231 *10, osm-7, osm-10, tax-2, tax-4, ttx-1(p767*), also had exploration defects but not as severe as
232 *grk-2*. Interestingly, chemosensory and osmosensory mutants *che-1, che-6, che-7, odr-2, odr-4,*
233 *odr-5, odr-7, osm-9,* and *osm-11*, as well as thermosensory *ttx-1(oy26* and *oy29)* mutants were
234 not significantly defective. Surprisingly, the *ocr-2* canonical null mutant *ak47* (VM396 strain)
235 showed an exploration defect that was not observed with the *ocr-2(ok1711)* allele (VC1233
236 strain). Given that *ok1711* contains a deletion of at least three exons it is presumably a null
237 allele, suggesting that either the VC1233 *ocr-2*(*ok1711)* strain has a suppressor mutation that
238 rescues the exploration defect or that the VM396 *ocr-2(ak47)* strain has an exploration defect
239 due to a background mutation and not because of the *ocr-2(ak47)* deletion. To distinguish
240 between these possibilities, we outcrossed strains VC1233 and VM396 and tested the
241 exploration behavior of outcrossed strains BJH2762 *ocr-2(ok1711)* and BJH2763 *ocr-2(ak47)*.
242 We found that strain BJH2763 *ocr-2(ak47)* did not have an exploration defect, suggesting that
243 the *ocr-2(ak47)* mutation does not cause exploration defects and that strain VM396 has a
244 background mutation that makes the animals exploration defective (Fig S3A). Notably, oxygen-
245 sensing mutant *gcy-35* and mechanosensory-defective mutants *mec-3, mec-4,* and *glr-1* did not

246 show exploration defects. We conclude that ciliated neurons that are involved in
247 chemosensation and osmosensation regulate the exploration behavior.
248
249 **GRK-2 regulates movement quiescence in an opposite way to EGL-4**
250 *C. elegans* locomotory behavior in the presence of food alternates between two discrete
251 states called roaming (exploring) and dwelling, where the animal either covers long distances or
252 explores locally, respectively [2,4]. The cGMP-dependent protein kinase EGL-4 acts in the
253 sensory neurons to promote dwelling [2]. *egl-4* loss of function mutant animals explore more
254 than wild type animals [2,4]. Also, *egl-4* mutations suppress the reduced exploration defect of
255 *che-2* mutants [2]. Thus, we examined whether *egl-4(n479)* mutant animals suppress the *grk-2*
256 exploration defect. We noticed that when the exploration assay was performed on 6 cm plates,
257 *egl-4* mutant animals didn't seem to explore significantly more than wild type animals, probably
258 due to a ceiling effect (Fig 4A). In contrast, when the assay was performed on 10 cm plates, *egl-*
259 *4* mutant animals explored significantly more than wild type animals (Fig 4B). In both cases, the
260 *egl-4(n479)* mutation significantly suppressed the *grk-2* exploration defect (Fig 4A,B).
261 Expression of EGL-4 in ciliated neurons reversed the *egl-4* suppression of the *grk-2* exploration
262 defect (Fig 4C), suggesting that GRK-2 and EGL-4 act in opposite ways in the ciliated neurons
263 to regulate exploration.
264 EGL-4 also functions in sensory neurons to promote a *C. elegans* sleep state during
265 lethargus (lethargus quiescence; [3]). The described role of EGL-4 in quiescence prompted us
266 to examine whether the exploration defect of *grk-2* is the result of movement quiescence. We
267 measured activity and quiescence in *C. elegans* larval stage 4 (L4) animals by imaging
268 individual animals cultivated in a WorMotel, which is a micro-fabricated device with multiple
269 agar-filled wells [47,48]. Single L4 animals were placed in WorMotel, imaged for 8 h, and their
270 quiescence and activity were quantified. *grk-2(gk268)* mutant animals showed reduced body
271 movement activity and increased quiescence in this 8 h period and the *egl-4(n479)* mutation

272 suppressed these phenotypes (Fig 4D-F). We conclude that *grk-2* mutant animals have
273 enhanced movement quiescence that is suppressed by *egl-4*, indicating that *grk-2* and *egl-4* act
274 in opposite directions to regulate movement quiescence. These results also suggest that part of
275 the exploration defect of *grk-2* mutant might be the result of increased movement quiescence.
276 In addition to cGMP signaling through EGL-4, cAMP signaling pathways act through the
277 salt-inducible kinase KIN-29 in sensory neurons to regulate sensory behaviors [49]. *kin-29* plays
278 an important role in the metabolic regulation of sleep [50] and *kin-29* mutants, like *egl-4*
279 mutants, have reduced sleep. However, in contrast to *egl-4* mutant animals, *kin-29(oy38)*
280 mutant animals did not explore more than wild-type animals and the *kin-29(oy38)* mutation did
281 not rescue the exploration defect of *grk-2(gk268)* mutant (Fig S3B). We conclude that KIN-29
282 does not play a role in the GRK-2 pathway to control exploration and movement quiescence.
283
284 **APTF-1 promotes GRK-2-modulated movement quiescence and exploration**
285 To further explore the role of sleep in the reduced exploration of *grk-2* mutant, we
286 manipulated sleep in *grk-2* mutant animals. Sleep behavior is controlled by the AP2 transcription
287 factor APTF-1, which is required for the development of the sleep-promoting RIS interneuron
288 [51]. Although the exploration behavior of *aptf-1(gk794)* mutant animals was similar to that of
289 wild type animals, the *aptf-1* mutation partially suppressed the decreased exploration phenotype
290 of *grk-2* mutant animals (Fig 5A). Similarly, *aptf-1* mutant partially suppressed both the
291 enhanced quiescence and reduced activity phenotypes of *grk-2* mutant (Fig 5B-D). We
292 conclude that increased sleep is partially responsible for the reduced exploration phenotype of
293 *grk-2* mutant animals.
294 APTF-1 promotes sleep by turning on the expression of the sleep-inducing neuropeptide
295 FLP-11 in the RIS neuron. At sleep onset, increases in RIS calcium activity cause the release of
296 FLP-11, which induces quiescence [9]. *flp-11(tm2706)* mutant did not significantly affect the
297 exploration or quiescence phenotypes of *grk-2* mutant (Fig S4A-D), suggesting that GRK-2 acts

298 independently of FLP-11 in regulating quiescence, and that the role of APTF-1 in adult
299 movement quiescence is partially independent of FLP-11. Alternatively, since the effect of *flp-11*
300 on sleep is weaker than that of *aptf-1* [9], our assays might not be sensitive enough to detect a
301 phenotype for *flp-11*.
302 *C. elegans* displays an additional sleep-like quiescent behavior which occurs in
303 response to exposure to cellular stressors (stress-induced quiescence). Mutants lacking the
304 transcription factor CEH-17 lack a functional ALA neuron, a neuron which promotes stress-
305 induced quiescenc [13,14,52,53]. In contrast to the *aptf-1* mutation, the *ceh-17(np1)* mutation
306 did not affect the exploration or quiescence phenotypes of *grk-2* (Fig S4E-H), suggesting that
307 GRK-2 acts independently of the ALA neuron to regulate movement quiescence.
308
309 **NPR-1 negatively regulates GRK-2- modulated exploration**
310 The *C. elegans* neuropeptide receptor NPR-1 negatively regulates arousal by inhibiting
311 the activity of a sensory circuit that is connected by gap junctions to the RMG interneurons [54].
312 *npr-1* loss-of-function mutant animals have increased locomotion both in lethargus and in the
313 adult stage due to heightened activity of the RMG circuit [8,30-32,54]. *npr-1(ky13)* mutant
314 animals explored more than wild type animals and *npr-1(ky13)* suppressed the exploration
315 defect of *grk-2(gk268)* (Fig 6A,B). Moreover, *npr-1(ky13)* also suppressed the *grk-2* dispersal
316 defect in the absence of food (Fig 6C). These results suggest that *npr-1* and *grk-2* act in
317 opposite ways to regulate exploration.
318 The FMRFamide-related neuropeptides (FaRPs) FLP-18 and FLP-21 are known NPR-1
319 ligands [55,56]. While *flp-18(db99)* and *flp-21(ok889)* single mutants did not have an exploration
320 defect, a *flp-18* mutation partially suppressed the defective exploration phenotype of *grk-2* (Fig
321 6D). The *flp-21* mutation did not affect the *grk-2* exploration defect and *flp-21; flp-18* mutants
322 were not stronger suppressors than *flp-18* mutants, suggesting that the *flp-21(ok889)* mutation
323 does not suppress the *grk-2* exploration defect (Fig 6E). The NPR-1 ligand FLP-18 only having

324 a partial effect suggests that it is not the only ligand for NPR-1 in this pathway. Alternatively,
325 NPR-1 may have ligand-independent activity.
326 NPR-1 is expressed in several neurons including neurons of the RMG circuit (ASH,
327 URX, RMG) [57] and expression in the RMG circuit completely rescues the increased
328 locomotion of *npr-1* mutants during lethargus [8,31]. Moreover, expression solely in the RMG
329 interneuron rescues the enhanced locomotion speed of *npr-1* mutants [54] while NPR-1 acts in
330 the ASH sensory neurons to inhibit sensory responses [8]. To examine whether ASH-specific
331 expression of *npr-1* is sufficient to reverse the *npr-1* suppression of the exploration defect of *grk-*
332 *2* mutants we expressed the *npr-1* cDNA under the control of the ASH (and ASI) - specific *sra-6*
333 promoter (*sra-6p*; [40]). Expression of *npr-1* under the *sra-6* promoter did not reverse the *npr-*
334 *1(ky13)* suppression of the exploration defect of *grk-2* (Fig 6F).
335 We next addressed whether RMG- specific expression of *npr-1* is sufficient to reverse
336 the *npr-1*- suppression of the exploration defect of *grk-2*. Since RMG- specific promoters are not
337 known, we used a described intersection strategy to drive *npr-1* expression only in the RMG
338 neuron [54]. In this approach, we used the *ncs-1* promoter to drive the Cre recombinase and the
339 *flp-21* promoter to drive *npr-1* preceded by a floxed STOP site. [54]. Expression of *npr-1* by this
340 method in *grk-2(gk268); npr-1(ky13)* mutant animals fully reversed the *npr-1* suppression of the
341 exploration defect of *grk-2* (Fig 6F). *flp-21* and *ncs-1* are coexpressed in several neurons
342 (including the RMG neurons), but of these neurons, *npr-1* is present only in ASE, ASG, and
343 RMG. Since ASE and ASG are gustatory neurons that have not been implicated in NPR-1
344 function in locomotion, our experiments suggest that NPR-1 functions in RMG to negatively
345 regulate the GRK-2 pathway that modulates exploration.
346
347 **FLP-1 negatively controls GRK-2- mediated exploration**
348 In a literature search for additional neuropeptides that could play a role in GRK-2-
349 modulated exploration, we came across FLP-1. *flp-1(ok2811)* null mutant animals are

350 hyperactive and have a loopy locomotion posture characterized by deep body bends [34-37].
351 Interestingly, although *flp-1(ok2811)* mutant animals explored as well as WT animals in the
352 presence of food, the *flp-1(ok2811)* mutation significantly suppressed the *grk-2(gk268)*
353 exploration defect (Fig 7A). Moreover, *grk-2(gk268); flp-1(ok2811); flp-18(db99)* triple mutant
354 animals behaved like the *grk-2(gk268); flp-1(ok2811)* double mutant, suggesting that FLP-1 and
355 FLP-18 act in the same pathway to negatively modulate GRK-2-mediated exploration (Fig 7B).
356 Expression of FLP-1 under its own promoter and under the AVK neuron-specific *twk-47*
357 promoter reversed the *flp-1* suppression of the *grk-2* exploration phenotype, suggesting that
358 expression of FLP-1 in AVK interneurons is sufficient to restore its function (Fig 7C). To assess
359 whether *npr-1* and *flp-1* act in the same pathway, we built the triple mutant *grk-2; flp-1; npr-1*
360 and compared its phenotype with that of the *grk-2; npr-1* double mutant. We found that *grk-2;*
361 *flp-1; npr-1* behaves like *grk-2; npr-1* mutant animals, suggesting that either NPR-1 and FLP-1
362 act in the same pathway or that we cannot detect further suppression due to a ceiling effect (Fig
363 7D,E). Previous reports suggest that NPR-6 and FRPR-7 are low- and high-affinity FLP-1
364 receptors, respectively [36]. We tested the exploration behavior of *grk-2(gk268); npr-6(tm1497)*
365 and *grk-2(gk268); frpr-7(gk463846)* double mutants. *npr-6(tm1497)* did not affect the exploration
366 behavior of *grk-2(gk268),* but *frpr-7(gk463846)* partially but significantly suppressed the
367 exploration defect of *grk-2(gk268)* (Fig 7F). These results suggest that *frpr-7* but not *npr-6* could
368 be playing a role in the exploration behavior.
369
370 **GRK-2 negatively regulates FLP-1 secretion from the AVK neuron**
371 To examine the possibility of a functional connection between GRK-2 and FLP-1, we
372 assessed whether GRK-2 affects the levels of FLP-1 secretion using the coelomocyte uptake
373 assay [58-60]. Proteins that are secreted into the *C. elegans* body cavity are endocytosed by
374 scavenger cells named coelomocytes (Fig 8A). We expressed the fusion protein FLP-
375 1::mCherry in AVK neurons of *flp-1* single mutant animals and of *grk-2; flp-1* double mutant

376 animals and quantified the intensity of fluorescence in coelomocytes as a readout of secreted
377 FLP-1::mCherry (see Methods; [36]). Previous work confirmed that FLP-1::mCherry follows the
378 dense core vesicle route for neuropeptide secretion and used the FLP-1::mCherry secretion
379 assay as a way of evaluating FLP-1 secretion [36]. Notably, FLP-1::mCherry expression in *grk-*
380 *2; flp-1* reversed the suppression of the exploration defect of *grk-2* by *flp-1,* suggesting that FLP-
381 1 in the FLP-1::mCherry reporter retains its function in exploration (Fig S5). *grk-2; flp-1* mutants
382 expressing FLP-1::mCherry had significantly increased levels of mCherry in coelomocytes in
383 comparison to *flp-1* mutant animals (Fig 8A,B). To examine whether background fluorescence in
384 the coelomocytes of *grk-2; flp-1* mutants also changed, together with FLP-1::mCherry we co-
385 expressed a reporter expressing GFP driven by the coelomocyte-specific promoter *unc-122* and
386 tested the levels of GFP fluorescence in the coelomocytes of *flp-1* and *grk-2; flp-1* mutants. We
387 found that GFP fluorescence remained unchanged in *grk-2; flp-1* mutants suggesting that the
388 increase in FLP-1::mCherry fluorescence in *grk-2; flp-1* coelomocytes is specific to FLP-
389 1::mCherry (Fig 8C). These results suggest that GRK-2 affects the level of secreted FLP-1,
390 which could explain at least in part the exploration defect observed in mutants lacking GRK-2.
391 Consistent with this idea, multi-copy expression of FLP-1::mCherry under the *flp-1* promoter
392 reduced the exploration behavior of wild type animals (Fig 8D). These results altogether indicate
393 that GRK-2 negatively regulates the amount of FLP-1 that is secreted by AVK neurons, resulting
394 in positive regulation of the exploration behavior.

395 **Discussion**

396 Locomotion is the result of dynamic interactions between a genetically determined
397 central program and feedback mechanisms that modulate the activity of the central program
398 [61]. Feedback is mainly of sensory and neuromodulatory nature and it plays a major role in
399 adapting the pattern of locomotion to environmental or metabolic changes [1]. Here we have
400 demonstrated that locomotor behavioral strategies in the nematode *Caenorhabditis elegans* are
401 altered through the action of the G protein-coupled receptor kinase-2 (GRK-2) in ciliated
402 sensory neurons and neuropeptide signaling in interneurons. We propose that GRK-2 acts in
403 ciliated sensory neurons to regulate exploration and the arousal state of the animal by
404 controlling the level of secretion of the neuropeptide FLP-1.

405

406 **GRK-2 signaling in ciliated sensory neurons controls exploration**

407 The sensory system influences the expression of different locomotor states in *C.*
408 *elegans*, like roaming and dwelling [2]. Roaming is a behavioral exploration strategy where the
409 animal covers long distances, while dwelling is a local search behavior strategy where animals
410 restrict their activity to a small region. Previous studies have shown that mutants with
411 diminished sensory responses to soluble and volatile chemicals are defective in the time they
412 spend roaming or dwelling, suggesting that sensory perception is critical for this behavior [2].
413 Specifically, a class of mutants that lack a normal sensory cilium structure, including *che-2*
414 [62,63], are unable to explore long distances. In this study we show that *grk-2* mutant animals
415 have similarly severe phenotypes as the cilium structure mutants in that they also show reduced
416 exploration. Our findings suggest that the positive role of GRK-2 in exploration is due to its
417 positive role in chemosensation. We show that expression of GRK-2 in the ciliated sensory
418 neurons of *grk-2* mutant animals rescues their exploration defect, suggesting that GRK-2 acts
419 specifically in these neurons to mediate exploration. Our effort to narrow down the specific
420 neurons where GRK-2 acts to mediate this behavior revealed that GRK-2 acts in multiple

421 ciliated neurons to control exploration. Interestingly, although *grk-2* mutant animals have strong
422 chemosensory defects, they do not have severe cilia structural defects like the cilium structure
423 mutants [23,64]. Also, expression of GRK-2 in adult *grk-2* mutant animals can rescue the *grk-2*
424 exploration defect suggesting that GRK-2 plays a non-developmental role in ciliated neurons to
425 promote exploration. Our study of mutants with defects in different kinds of sensory perception
426 showed that the activity of the ciliated neurons that are involved in chemosensation and
427 osmosensation regulate the exploration behavior, but neurons involved in mechanosensation or
428 oxygen-sensation do not. These results together suggest that impaired sensory neuron function
429 per se can reduce exploration.

430 Our results show that *grk-2* and the cilium structure mutant *che-2* act in the same
431 genetic pathway to regulate exploration, again suggesting that impaired ciliated sensory neuron
432 function disrupts exploration. In agreement, we found that mutations in the gene encoding the
433 cGMP-dependent protein kinase EGL-4 that suppress the altered exploration behavior of *che-2*
434 mutants [2], also suppress the exploration defect of *grk-2* mutant animals. Given that expression
435 of EGL-4 in the ciliated neurons reverses this suppression, we propose that both GRK-2 and
436 EGL-4 act in ciliated neurons to control exploration but in opposite ways. We do not yet know
437 whether the two kinases act in the same ciliated neurons to control exploration. Given that both
438 GRK-2 and EGL-4 act in multiple ciliated neurons to regulate exploration and that other
439 chemosensory and osmosensory mutants have similar exploration defects as *grk-2*, we support
440 a model in which GRK-2 acts in ciliated neurons to positively control sensory perception and
441 affect the exploration state of the animal by regulating EGL-4. We propose that in *grk-2* and
442 cilium structure mutants, impaired sensory perception leads to increase in EGL-4 activity and
443 decreased exploration. A similar model was supported by previous studies, which showed that
444 EGL-4 regulates body size and locomotory states in a way depending on sensory perception [2].
445 Alternatively, the two kinases GRK-2 and EGL-4, might act in different ciliated neurons, leading
446 to opposite outcomes in sensory perception and exploration.

447 In previous work we have shown that GRK-2 regulates crawling and swimming [27,28]
448 by possibly phosphorylating the D2-like dopamine receptor DOP-3 in premotor interneurons (Fig
449 9A). In the case of chemosensation and exploration, the target(s) of GRK-2, which are located
450 in chemosensory neurons and not interneurons, are currently unknown (Fig 9B). Similarly, we
451 do not yet know the identity of the phosphorylation target(s) for EGL-4.
452
453 **GRK-2 controls movement quiescence**
454 Animals undergo periods of quiescence and arousal in response to changes in their
455 environment or metabolic state. For example, *C. elegans* increases its exploration behavior
456 when it is removed from food [10,11] and shows quiescence during larval molting (lethargus)
457 and under starvation, satiety, and stress [3,12-17]. The cGMP-dependent protein kinase EGL-4
458 acts in sensory neurons to promote *C. elegans* sleep where the animals become quiescent
459 during lethargus [3]. This result, together with the observed opposite functionality between EGL-
460 4 and GRK-2 in ciliated neurons prompted us to examine whether *grk-2* mutants have
461 movement quiescence defects. Indeed, we found that *grk-2* mutant animals have enhanced
462 movement quiescence, which is suppressed by *egl-4*. This result suggests that GRK-2 and
463 EGL-4 act antagonistically to control movement quiescence outside lethargus. We propose that
464 GRK-2 acts in ciliated neurons to control sensory perception and affect movement quiescence
465 by negatively regulating EGL-4. Our findings imply that the exploration defect of *grk-2* and other
466 chemosensory mutants besides *grk-2* might be due in part to enhanced movement quiescence.
467 This series of data also suggests that *C. elegans* locomotion strategies that have been
468 described as exploration, roaming, and arousal might reflect the same behavior.
469 In addition to EGL-4, the AP2 transcription factor APTF-1 also plays an important role in
470 regulating sleep, largely by regulating expression of the sleep-inducing neuropeptide FLP-11 in
471 the RIS interneuron [51]. Indeed, we found that *aptf-1* mutants partially suppress the decreased
472 exploration phenotype, enhanced quiescence, and reduced activity of *grk-2*. This result

473 suggests that increased sleep is partially responsible for the reduced exploration phenotype of
474 *grk-2* mutant animals. Surprisingly, we found that *flp-11* mutations do not suppress the
475 enhanced quiescence of *grk-2* mutant animals. One possible explanation is that APTF-1 acts
476 through additional targets besides FLP-11, which is also supported by previous studies [9].
477 Alternatively, FLP-11 might be playing a smaller role than APTF-1 in adult quiescence and our
478 assays might not be sensitive enough to detect it.
479
480 **Neuromodulation through FLP-1 negatively regulates exploration**
481 Mutants lacking the neuropeptide receptor NPR-1 have been described as a model for
482 arousal both during lethargus and in adults [8,31-33]. NPR-1 is proposed to act in the RMG
483 interneuron to inhibit the activity of a sensory circuit that is connected to RMG via gap junctions
484 (54). In *npr-1* mutants, enhanced sensory activity causes aroused locomotion [8,31-33,65]. Our
485 results show that *npr-1* mutants suppress the exploration defects of *grk-2* mutant animals, and
486 that NPR-1 acts in RMG neurons to mediate this effect. The fact that *npr-1* is epistatic to *grk-2*
487 suggests that GRK-2 negatively regulates NPR-1 – in a *grk-2* mutant, increase in NPR-1 activity
488 inhibits exploration (Fig 9B). Of the reported NPR-1 ligands FLP-18 and FLP-21, we found that
489 only FLP-18 acts in the GRK-2 pathway that mediates exploration, since *flp-18* mutants partially
490 suppress the exploration defect of *grk-2* [55,56]. Interestingly, we also found that mutants in the
491 gene encoding the neuropeptide FLP-1 partially suppress the *grk-2* exploration defect and that
492 FLP-1 acts in the same genetic pathway as FLP-18. FLP-1 has not been reported to be a
493 ligand for *C. elegans* NPR-1, but it was shown to activate the *Girardia tigrina* neuropeptide
494 receptor 1 GtNPR-1 when expressed in Chinese hamster ovary cells [66]. This finding together
495 with our genetic observations could suggest that FLP-1 directly acts through NPR-1 to affect
496 exploration. Alternatively, and since *flp-1* and *flp-18* mutants do not act in an additive way to
497 suppress the *grk-2* exploration defect, FLP-1 could be acting in the GRK-2 pathway through a

498 different receptor than NPR-1. The partial suppression of the *grk-2* exploration defect by *frpr-7*,
499 suggests that the high-affinity FLP-1 receptor FRPR-7 could be playing a role.
500 Notably, Oranth et al (2018) [36] suggested that after >10 min off food, AVK releases
501 FLP-1 peptides to promote dispersal. Our genetic experiments show that mutants in *flp-1*
502 suppress the exploration defect of *grk-2* mutant animals and that overexpression of FLP-1
503 reduces exploration in the presence of food. This apparent discrepancy might be attributed to
504 different FLP-1 functionality in the presence or absence of food or when chemosensation is
505 impaired. Our genetic results together with our finding that GRK-2 modulates the secretion
506 levels of FLP-1 suggest that GRK-2, negatively regulates FLP-1 secretion, either directly or
507 indirectly (Fig 9B). Since GRK-2 acts in ciliated neurons to affect exploration and GRK-2
508 modulates FLP-1 secretion from AVK neurons we propose that GRK-2 acts in ciliated neurons
509 to mediate FLP-1 secretion from AVKs in a non-cell autonomous way. Given that there is no
510 known synaptic input from chemosensory neurons to AVKs [67] we suggest that GRK-2-driven
511 regulation of sensory neuron activity affects a neuromodulatory pathway that drives FLP-1
512 secretion from AVKs (Fig 9B). Alternatively, GRK-2 action in ciliated neurons may lead to
513 modulation of the neuronal circuit downstream of the ciliated neurons that eventually affects
514 secretion of FLP-1. According to our model, GRK-2 activity positively regulates chemosensory
515 neuron activity, which in turn inhibits EGL-4 activity, modulating exploration and the arousal
516 state of *C. elegans* through neuromodulatory signaling acting in interneurons (Fig 9B). Thus, an
517 active chemosensory system can guide *C. elegans* towards exploration, while a defective
518 chemosensory system inhibits dispersal and puts the animal in a state of quiescence.

519 **Methods**

520 **Strains**

521 Strains were maintained at room temperature or 20° on the OP50 strain of *E. coli* [68].
522 The Supplementary Information contains a list of strains used, including their full genotypes (S1
523 Table; List of strains).

524

525 **Constructs and transgenes**

526 The Supplementary Information contains a list of constructs used (S2 Table; List of
527 plasmids). All constructs made in this study were constructed using the Gateway system
528 (Invitrogen): a promoter region, a gene region (cDNA) or fluorescent tag, and a N- or C-terminal
529 3'UTR or fluorescent tag fused to a 3'UTR were cloned into the destination vector pCFJ150 [69].
530 For the cell-specific rescuing experiments, an operon GFP was included in the expression
531 constructs downstream of the 3'UTR [70]. This resulted in expression of untagged protein, but
532 also allowed for confirmation of proper promoter expression by monitoring GFP expression.

533 Extrachromosomal arrays were made by standard injection and transformation methods
534 [71]. We injected 5-10 ng/ul of the expression plasmid for *grk-2* and *flp-1* rescue experiments
535 and 20 ng/ul of the plasmids for other experiments. For the *yakEx261* FLP-1 overexpression
536 experiment in Fig 8D we injected 60 ng/ul. We injected 50 ng/ul of the *unc-122*::GFP co-
537 injection marker, 1 ng/ul of *myo-2p*::mCherry, 5 ng/ul of *myo-3p*::mCherry, and 5 ng/ul of *rab-*
538 *3p*::mCherry. We isolated two to three independent lines and tested two lines. The results
539 shown in the figures are for one of the lines tested.

540

541 **Exploration assays**

542 The exploration assay is an established assay that measures the ability of the animals to
543 explore (wander) during long periods of time [4]. Exploration assays were performed on 6 or 10
544 cm nematode growth medium (NGM) plates uniformly seeded with 200 or 500 ul of the OP50

545 strain of *E. coli*, respectively, and spread with a glass spreader. 10 cm plates were used in the
546 case of mutants that explore more than wild type animals (e.g. *egl-4, npr-1*) in order to avoid a
547 ceiling effect because wild type animals usually explore most of the area of a 6 cm plate in a
548 20h period. Bacteria were grown on the NGM agar surface at room temperature for
549 approximately 48 h and the plates were stored at 4°C until needed. On the day of the
550 experiment, individual first-day adult animals were transferred to the center of each plate and
551 were allowed to explore for 18-20 h. Then the plates were superimposed on a 50- or 150-
552 square grid and we counted the number of squares entered by the worm tracks. Approximately
553 5-30 animals were tested per strain. Every strain was tested on two independent trials. The
554 number "n" in figure legends indicates the total number of animals sampled (animals from two
555 different trials are combined).
556
557 **Dispersal assays**
558 The dispersal (or radial locomotion) assay is an established assay that measures the
559 distance animals travel from the middle of the plate in a period [38]. Since the dispersal assay
560 measures distance, it is only performed for short periods of time (1h on food or 20 min on plates
561 without food). Dispersal assays were performed on 10 cm nematode growth medium (NGM)
562 plates that were uniformly seeded with 500 µl of the OP50 strain of *E. coli* and spread with a
563 glass spreader. Bacteria were grown at room temperature for approximately 48 h and the plates
564 were stored at 4°C until needed. Approximately 20 first day adult animals were transferred to the
565 center of a plate and were allowed to explore for 1 h. Then the positions of the worms were
566 marked and the distances of the worms from the starting point were measured. Dispersal
567 assays without food were performed on NGM plates that were not spread with OP50 and the
568 animals were allowed to move freely for 20 min. Animals were first transferred to an
569 intermediate plate without food before being transferred to the assay plate. Approximately 20-40
570 animals were tested per strain. Every strain was tested on two independent trials. The number

571 “n” in figure legends indicates the total number of animals sampled (animals from the different
572 trials are combined).
573
574 **Heat shock assay**
575 Animals were raised to young adulthood at room temperature (23°C), then shifted to
576 34°C for 2 hr. They were allowed to recover at room temperature (23°C) for 4 hr and tested.
577
578 **Movement quiescence assays**
579 Movement quiescence assays were performed as previously described [48]. Briefly,
580 animals were selected as fourth larval stage L4s the day prior to the assay. They were loaded
581 individually onto the surface of NGM agar-filled wells on a PDMS WorMotel chip. The agar
582 surface in each well was covered in a thin lawn of DA837 *E. coli*. The loaded chip was placed in
583 a 10 cm petri dish lined with damp kimwipes to prevent desiccation and placed under a camera.
584 Behavior was recorded for eight hours with an image acquired every 10 seconds. The images
585 were then analyzed using a custom written program in Matlab. For more details on this method
586 see [48]. Approximately 10 animals were tested per experiment and per strain. The “n” in figure
587 legends indicates the total number of animals sampled.
588
589 **Body bend locomotion assay**
590 First-day adults were picked to a three-day-old lawn of OP50 and stimulated by poking
591 the tail of the animal with a worm pick. Body bends were then immediately counted for one
592 minute. A body bend was defined as the movement of the worm from maximum to minimum
593 amplitude of the sine wave. Approximately 10 animals were tested per strain. Every strain was
594 tested on two independent trials. The number “n” in figure legends indicates the total number of
595 animals sampled (animals from the different trials are combined).
596

597 **Imaging**

598 For fluorescence imaging, first-day adult animals were mounted on 2% agarose pads
599 and anesthetized with 50 mM sodium azide for ten minutes before placing the cover slip. The
600 animals were imaged using an Olympus FLUOVIEW FV1200 confocal microscope with a 60×
601 UPlanSApo oil objective (NA = 1.35) or a NikonTi2-E Crest X-light V2 spinning disk confocal
602 with a 60x oil objective (NA = 1.4).

603

604 **Coelomocyte assay**

605 For coelomocyte imaging we used FLP-1::mCherry (a gift from Alexander Gottschalk;
606 [36]). We imaged the anterior coelomocytes in day 1 adults using a NikonTi2-E Crest X-light V2
607 spinning disk confocal with a 60x oil 1.4 NA objective. Maximum intensity projections of image
608 stacks were obtained using FluoView software (Nikon). For quantification, the maximum
609 fluorescence intensity was calculated using Fiji and the background fluorescence intensity was
610 subtracted to obtain coelomocyte fluorescence.

611

612 **Statistics**

613 Statistical analysis and graphing were carried out using Prism 8 or Prism 9 (GraphPad
614 Software). Normally distributed data sets requiring multiple comparisons were analyzed by a
615 one-way ANOVA or by a one-way ANOVA followed by a Bonferroni test. Normally distributed
616 pairwise data comparisons were analyzed by two-tailed unpaired t tests. $p < 0.05$ (following
617 Bonferroni correction, when appropriate) was considered to be statistically significant (*$p < 0.05$,
618 **$p < 0.01$, ***$p < 0.001$, ****$p<0.0001$). Data are presented as the mean ± standard error
619 (SEM).

620 **Raw data**

621 S3 Table contains all the data points used for the main and supplementary figures.

Acknowledgements

We dedicate this paper to the memory of Giannis Topalidis whose support was instrumental for the completion of this manuscript. Special thanks to Alexander Gottschalk for the FLP-1::mCherry plasmid, Ithai Rabinowitch for the *str-1, str-2,* and *odr-10* promoter plasmids, and Cori Bargmann for the pEM01 and pEM03 plasmids. Some strains were provided by the CGC, which is funded by the NIH Office of Research Infrastructure Programs (P40 OD010440). This work was funded by R01 NS109476 to MA and JB, R01 GM121481 to MA, R01 NS122779 and R01 NS107969 to DMR. KT was supported by a T32Act ES019851 Training grant (PI: Trever Penning).

Author contributions

KD and IT conceived the experiments. KD and IT performed the experiments and analyzed the data. CM and OP performed the experiments described in Fig 3D. MA, DMR, and JB assisted with providing ideas. IT wrote the paper with help from MA, DMR, and JB.

637 **References**

638 1. MacKay-Lyons M. Central pattern generation of locomotion: a review of the evidence. Phys
639 Ther. 2002 Jan;82(1):69–83.

640 2. Fujiwara M, Sengupta P, McIntire SL. Regulation of body size and behavioral state of *C.*
641 *elegans* by sensory perception and the EGL-4 cGMP-dependent protein kinase. Neuron.
642 2002 Dec 19;36(6):1091–102.

643 3. Raizen DM, Zimmerman JE, Maycock MH, Ta UD, You Y jai, Sundaram MV, et al.
644 Lethargus is a *Caenorhabditis elegans* sleep-like state. Nature. 2008 Jan
645 31;451(7178):569–72.

646 4. Flavell SW, Pokala N, Macosko EZ, Albrecht DR, Larsch J, Bargmann CI. Serotonin and
647 the neuropeptide PDF initiate and extend opposing behavioral states in *C. elegans*. Cell.
648 2013 Aug 29;154(5):1023–35.

649 5. Flavell SW, Raizen DM, You YJ. Behavioral States. Genetics. 2020 Oct;216(2):315–32.

650 6. Flavell SW, Gordus A. Dynamic functional connectivity in the static connectome of
651 *Caenorhabditis elegans*. Curr Opin Neurobiol. 2022 Feb 17;73:102515.

652 7. Taghert PH, Nitabach MN. Peptide neuromodulation in invertebrate model systems.
653 Neuron. 2012 Oct 4;76(1):82–97.

654 8. Choi S, Taylor KP, Chatzigeorgiou M, Hu Z, Schafer WR, Kaplan JM. Sensory Neurons
655 Arouse *C. elegans* Locomotion via Both Glutamate and Neuropeptide Release. PLoS
656 Genet. 2015 Jul;11(7):e1005359.

657 9. Turek M, Besseling J, Spies JP, König S, Bringmann H. Sleep-active neuron specification
658 and sleep induction require FLP-11 neuropeptides to systemically induce sleep. eLife.
659 2016 Mar 7;5:e12499.

660 10. Gray JM, Hill JJ, Bargmann CI. A circuit for navigation in *Caenorhabditis elegans.* Proc
661 Natl Acad Sci U S A. 2005 Mar 1;102(9):3184–91.

662 11. Hills T, Brockie PJ, Maricq AV. Dopamine and glutamate control area-restricted search
663 behavior in *Caenorhabditis elegans.* J Neurosci. 2004 Feb 4;24(5):1217-25.

664 12. You Y jai, Kim J, Raizen DM, Avery L. Insulin, cGMP, and TGF-beta signals regulate food
665 intake and quiescence in *C. elegans*: a model for satiety. Cell Metab. 2008 Mar;7(3):249–
666 57.

667 13. Hill AJ, Mansfield R, Lopez JMNG, Raizen DM, Van Buskirk C. Cellular stress induces a
668 protective sleep-like state in *C. elegans*. Curr Biol CB. 2014 Oct 20;24(20):2399–405.

669 14. Nelson MD, Lee KH, Churgin MA, Hill AJ, Van Buskirk C, Fang-Yen C, et al. FMRFamide-
670 like FLP-13 neuropeptides promote quiescence following heat stress in *Caenorhabditis*
671 *elegans*. Curr Biol CB. 2014 Oct 20;24(20):2406–10.

672 15. DeBardeleben HK, Lopes LE, Nessel MP, Raizen DM. Stress-Induced Sleep After
673 Exposure to Ultraviolet Light Is Promoted by p53 in *Caenorhabditis elegans*. Genetics.
674 2017 Oct;207(2):571–82.

675 16. Skora S, Mende F, Zimmer M. Energy Scarcity Promotes a Brain-wide Sleep State
676 Modulated by Insulin Signaling in *C. elegans*. Cell Rep. 2018 Jan 23;22(4):953–66.

677 17. Wu Y, Masurat F, Preis J, Bringmann H. Sleep Counteracts Aging Phenotypes to Survive
678 Starvation-Induced Developmental Arrest in *C. elegans.* Curr Biol CB. 2018 Nov
679 19;28(22):3610-3624.e8.

680 18. Daniels SA, Ailion M, Thomas JH, Sengupta P. *egl-4* acts through a transforming growth
681 factor-beta/SMAD pathway in *Caenorhabditis elegans* to regulate multiple neuronal circuits
682 in response to sensory cues. Genetics. 2000 Sep;156(1):123–41.

683 19. L'Etoile ND, Coburn CM, Eastham J, Kistler A, Gallegos G, Bargmann CI. The cyclic GMP-
684 dependent protein kinase EGL-4 regulates olfactory adaptation in *C. elegans.* Neuron.
685 2002 Dec 19;36(6):1079–89.

686 20. McCloskey RJ, Fouad AD, Churgin MA, Fang-Yen C. Food responsiveness regulates
687 episodic behavioral states in *Caenorhabditis elegans.* J Neurophysiol. 2017 May
688 1;117(5):1911–34.

689 21. Gurevich VV, Gurevich EV. GPCR Signaling Regulation: The Role of GRKs and Arrestins.
690 Front Pharmacol. 2019;10:125.

691 22. Gurevich EV, Tesmer JJG, Mushegian A, Gurevich VV. G protein-coupled receptor
692 kinases: more than just kinases and not only for GPCRs. Pharmacol Ther. 2012
693 Jan;133(1):40–69.

694 23. Fukuto HS, Ferkey DM, Apicella AJ, Lans H, Sharmeen T, Chen W, et al. G protein-
695 coupled receptor kinase function is essential for chemosensation in *C. elegans.* Neuron.
696 2004 May 27;42(4):581–93.

697 24. Wood JF, Wang J, Benovic JL, Ferkey DM. Structural domains required for *Caenorhabditis*
698 *elegans* G protein-coupled receptor kinase 2 (GRK-2) function in vivo. J Biol Chem. 2012
699 Apr 13;287(16):12634–44.

700 25. Hukema RK, Rademakers S, Dekkers MPJ, Burghoorn J, Jansen G. Antagonistic sensory
701 cues generate gustatory plasticity in *Caenorhabditis elegans*. EMBO J. 2006 Jan
702 25;25(2):312–22.

703 26. Wang J, Luo J, Aryal DK, Wetsel WC, Nass R, Benovic JL. G protein-coupled receptor
704 kinase-2 (GRK-2) regulates serotonin metabolism through the monoamine oxidase AMX-2
705 in *Caenorhabditis elegans.* J Biol Chem. 2017 Apr 7;292(14):5943–56.

706 27. Topalidou I, Cooper K, Pereira L, Ailion M. Dopamine negatively modulates the NCA ion
707 channels in *C. elegans*. PLoS Genet. 2017 Oct;13(10):e1007032.

708 28. Xu Y, Zhang L, Liu Y, Topalidou I, Hassinan C, Ailion M, et al. Dopamine receptor DOP-1
709 engages a sleep pathway to modulate swimming in *C. elegans.* iScience. 2021 Apr
710 23;24(4):102247.

711 29. Heilman C, Ibarreta J, Salonga GA, Hon MC, Caracci AM, Badial T, et al. G protein
712 coupled receptor kinases modulate *Caenorhabditis elegans* reactions to heat stresses.
713 Biochem Biophys Res Commun. 2020 Oct 1;530(4):692–8.

714 30. Henry SA, Crivello S, Nguyen TM, Cybulska M, Hoang NS, Nguyen M, et al. G protein-
715 coupled receptor kinase 2 modifies the ability of *Caenorhabditis elegans* to survive
716 oxidative stress. Cell Stress Chaperones. 2021 Jan;26(1):187–97.

717 31. Choi S, Chatzigeorgiou M, Taylor KP, Schafer WR, Kaplan JM. Analysis of NPR-1 reveals
718 a circuit mechanism for behavioral quiescence in *C. elegans*. Neuron. 2013 Jun
719 5;78(5):869–80.

720 32. Nichols ALA, Eichler T, Latham R, Zimmer M. A global brain state underlies *C. elegans*
721 sleep behavior. Science. 2017 Jun 23;356(6344):eaam6851.

722 33. Soto R, Goetting DL, Van Buskirk C. NPR-1 Modulates Plasticity in *C. elegans* Stress-
723 Induced Sleep. iScience. 2019 Sep 27;19:1037–47.

724 34. Hums I, Riedl J, Mende F, Kato S, Kaplan HS, Latham R, et al. Regulation of two motor
725 patterns enables the gradual adjustment of locomotion strategy in *Caenorhabditis elegans.*
726 eLife. 2016 May 25;5:e14116.

727 35. Buntschuh I, Raps DA, Joseph I, Reid C, Chait A, Totanes R, et al. FLP-1 neuropeptides
728 modulate sensory and motor circuits in the nematode *Caenorhabditis elegans.* PloS One.
729 2018;13(1):e0189320.

730 36. Oranth A, Schultheis C, Tolstenkov O, Erbguth K, Nagpal J, Hain D, et al. Food Sensation
731 Modulates Locomotion by Dopamine and Neuropeptide Signaling in a Distributed Neuronal
732 Network. Neuron. 2018 Dec 19;100(6):1414-1428.e10.

733 37. Topalidou I. Background mutation in strain RB2126 affects the locomotion behavior of *flp-1*
734 mutants. MicroPublication Biol. 2021 May 9;2021.

735 38. Coleman B, Topalidou I, Ailion M. Modulation of Gq-Rho Signaling by the ERK MAPK
736 Pathway Controls Locomotion in *Caenorhabditis elegans.* Genetics. 2018 Jun;209(2):523–
737 35.

738 39. Roayaie K, Crump JG, Sagasti A, Bargmann CI. The G alpha protein ODR-3 mediates
739 olfactory and nociceptive function and controls cilium morphogenesis in *C. elegans*
740 olfactory neurons. Neuron. 1998 Jan;20(1):55–67.

741 40. Troemel ER, Chou JH, Dwyer ND, Colbert HA, Bargmann CI. Divergent seven
742 transmembrane receptors are candidate chemosensory receptors in *C. elegans.* Cell. 1995
743 Oct 20;83(2):207–18.

744 41. Sengupta P, Chou JH, Bargmann CI. *odr-10* encodes a seven transmembrane domain
745 olfactory receptor required for responses to the odorant diacetyl. Cell. 1996 Mar
746 22;84(6):899–909.

747 42. Troemel ER, Kimmel BE, Bargmann CI. Reprogramming chemotaxis responses: sensory
748 neurons define olfactory preferences in *C. elegans.* Cell. 1997 Oct 17;91(2):161–9.

749 43. Troemel ER, Sagasti A, Bargmann CI. Lateral signaling mediated by axon contact and
750 calcium entry regulates asymmetric odorant receptor expression in *C. elegans.* Cell. 1999
751 Nov 12;99(4):387–98.

752 44. Yu S, Avery L, Baude E, Garbers DL. Guanylyl Cyclase expression in specific sensory
753 neurons: a new family of chemosensory receptors. Proc Natl Acad Sci U S A. 1997 Apr
754 1;94(7):3384–7.

755 45. Flames N, Hobert O. Gene regulatory logic of dopamine neuron differentiation. Nature.
756 2009 Apr 1;458(7240):885–9.

757 46. Inglis PN, Ou G, Leroux MR, Scholey JM. The sensory cilia of *Caenorhabditis elegans.*
758 2007 Mar 8; WormBook, ed. The *C. elegans* Research Community, WormBook. Available
759 from: http://www.wormbook.org

760 47. Churgin MA, Jung SK, Yu CC, Chen X, Raizen DM, Fang-Yen C. Longitudinal imaging of
761 *Caenorhabditis elegans* in a microfabricated device reveals variation in behavioral decline
762 during aging. eLife. 2017 May 31;6:e26652.

763 48. Churgin MA, Szuperak M, Davis KC, Raizen DM, Fang-Yen C, Kayser MS. Quantitative
764 imaging of sleep behavior in *Caenorhabditis elegans* and larval Drosophila melanogaster.
765 Nat Protoc. 2019 May;14(5):1455–88.

766 49. van der Linden AM, Wiener S, You Y jai, Kim K, Avery L, Sengupta P. The EGL-4 PKG
767 acts with KIN-29 salt-inducible kinase and protein kinase A to regulate chemoreceptor
768 gene expression and sensory behaviors in *Caenorhabditis elegans.* Genetics. 2008
769 Nov;180(3):1475–91.

770 50. Grubbs JJ, Lopes LE, van der Linden AM, Raizen DM. A salt-induced kinase is required for
771 the metabolic regulation of sleep. PLoS Biol. 2020 Apr;18(4):e3000220.

772 51. Turek M, Lewandrowski I, Bringmann H. An AP2 transcription factor is required for a sleep-
773 active neuron to induce sleep-like quiescence in *C. elegans.* Curr Biol CB. 2013 Nov
774 18;23(22):2215–23.

775 52. Pujol N, Torregrossa P, Ewbank JJ, Brunet JF. The homeodomain protein
776 CePHOX2/CEH-17 controls antero-posterior axonal growth in *C. elegans.* Dev Camb Engl.
777 2000 Aug;127(15):3361–71.

778 53. Trojanowski NF, Nelson MD, Flavell SW, Fang-Yen C, Raizen DM. Distinct Mechanisms
779 Underlie Quiescence during Two *Caenorhabditis elegans* Sleep-Like States. J Neurosci
780 Off J Soc Neurosci. 2015 Oct 28;35(43):14571–84.

781 54. Macosko EZ, Pokala N, Feinberg EH, Chalasani SH, Butcher RA, Clardy J, et al. A hub-
782 and-spoke circuit drives pheromone attraction and social behaviour in *C. elegans.* Nature.
783 2009 Apr 30;458(7242):1171–5.

784 55. Kubiak TM, Larsen MJ, Nulf SC, Zantello MR, Burton KJ, Bowman JW, et al. Differential
785 activation of "social" and "solitary" variants of the *Caenorhabditis elegans* G protein-
786 coupled receptor NPR-1 by its cognate ligand AF9. J Biol Chem. 2003 Sep
787 5;278(36):33724–9.

788 56. Rogers C, Reale V, Kim K, Chatwin H, Li C, Evans P, et al. Inhibition of *Caenorhabditis*
789 *elegans* social feeding by FMRFamide-related peptide activation of NPR-1. Nat Neurosci.
790 2003 Nov;6(11):1178–85.

791 57. Coates JC, de Bono M. Antagonistic pathways in neurons exposed to body fluid regulate
792 social feeding in *Caenorhabditis elegans*. Nature. 2002 Oct 31;419(6910):925–9.

793 58. Fares H, Greenwald I. Genetic analysis of endocytosis in *Caenorhabditis elegans:*
794 coelomocyte uptake defective mutants. Genetics. 2001 Sep;159(1):133–45.

795 59. Sieburth D, Madison JM, Kaplan JM. PKC-1 regulates secretion of neuropeptides. Nat
796 Neurosci. 2007 Jan;10(1):49–57.

797 60. Speese S, Petrie M, Schuske K, Ailion M, Ann K, Iwasaki K, et al. UNC-31 (CAPS) Is
798 Required for Dense-Core Vesicle But Not Synaptic Vesicle Exocytosis in *Caenorhabditis*
799 *elegans.* J Neurosci. 2007 Jun 6;27(23):6150–62.

800 61. Rossignol S, Dubuc R, Gossard JP. Dynamic sensorimotor interactions in locomotion.
801 Physiol Rev. 2006 Jan;86(1):89–154.

802 62. Lewis JA, Hodgkin JA. Specific neuroanatomical changes in chemosensory mutants of the
803 nematode *Caenorhabditis elegans.* J Comp Neurol. 1977 Apr 1;172(3):489–510.

804 63. Perkins LA, Hedgecock EM, Thomson JN, Culotti JG. Mutant sensory cilia in the nematode
805 *Caenorhabditis elegans.* Dev Biol. 1986 Oct;117(2):456–87.

806 64. Mukhopadhyay S, Lu Y, Shaham S, Sengupta P. Sensory signaling-dependent remodeling
807 of olfactory cilia architecture in *C. elegans.* Dev Cell. 2008 May;14(5):762–74.

808 65. Nagy S, Tramm N, Sanders J, Iwanir S, Shirley IA, Levine E, et al. Homeostasis in *C.*
809 *elegans* sleep is characterized by two behaviorally and genetically distinct mechanisms.
810 eLife. 2014 Dec 4;3:e04380.

811 66. Omar HH, Humphries JE, Larsen MJ, Kubiak TM, Geary TG, Maule AG, et al. Identification
812 of a platyhelminth neuropeptide receptor. Int J Parasitol. 2007 Jun;37(7):725–33.

813 67. White JG, Southgate E, Thomson JN, Brenner S. The structure of the nervous system of
814 the nematode *Caenorhabditis elegans.* Philos Trans R Soc Lond B Biol Sci. 1986 Nov
815 12;314(1165):1–340.

816 68. Brenner S. The genetics of *Caenorhabditis elegans.* Genetics. 1974 May;77(1):71–94.

817 69. Frøkjær-Jensen C, Davis MW, Sarov M, Taylor J, Flibotte S, LaBella M, et al. Random and
818 targeted transgene insertion in *Caenorhabditis elegans* using a modified Mos1 transposon.
819 Nat Methods. 2014 May;11(5):529–34.

820 70. Frøkjær-Jensen C, Davis MW, Ailion M, Jorgensen EM. Improved Mos1-mediated
821 transgenesis in *C. elegans.* Nat Methods. 2012 Jan 30;9(2):117–8.

822 71. Mello CC, Kramer JM, Stinchcomb D, Ambros V. Efficient gene transfer in *C.elegans*:
823 extrachromosomal maintenance and integration of transforming sequences. EMBO J. 1991
824 Dec;10(12):3959–70.

825

826

827 **Figure captions**

828 **Fig 1. *grk-2* mutant animals have dispersal and exploration defects.**

829 (A) Schematic representation of the assay used to measure dispersal (see Methods).

830 (B) *grk-2(gk268)* mutant animals have a dispersal defect in the presence of food and *dop-*

831 *3(vs106)* does not rescue this phenotype. Shown is the distance (cm) animals traveled from the

832 center of the plate in the presence of food in 1 h. (****, P<0.0001. ns, P>0.05. One way ANOVA

833 followed by a Bonferroni test. Error bars = SEM; n = 22–53).

834 (C) *grk-2(gk268)* mutant animals have a dispersal defect in the absence of food and *dop-*

835 *3(vs106)* does not rescue this phenotype. Shown is the distance (cm) animals traveled from the

836 center of the plate without food in 20 min. (****, P<0.0001. ns, P>0.05. One way ANOVA

837 followed by a Bonferroni test. Error bars = SEM; n = 47-60).

838 (D) Schematic representation of the assay used to measure exploration (see Methods).

839 (E) *grk-2(gk268)* mutant hermaphrodites have an exploration defect and *dop-3(vs106)* does not

840 rescue this defect. Shown is the number of squares (out of 50) single animals covered in

841 approximately 20 h. (****, P<0.0001. ns, P>0.05. One way ANOVA followed by a Bonferroni

842 test. Error bars = SEM; n = 15-18).

843 (F) *grk-2(gk268)* mutant males have an exploration defect. (****, P<0.0001. Student's t-test.

844 Error bars = SEM; n = 20-21).

845

846 **Fig 2. *grk-2* acts in the ciliated neurons to control exploration.**

847 (A) Expression of *grk-2* cDNA under a pan-neuronal promoter rescues the exploration defect of

848 *grk-2* mutant animals in the presence of food. The *grk-2* cDNA was expressed in *grk-2(gk268)*

849 mutant animals under a pan-neuronal promoter (*rab-3p*, transgene *yakEx44*), ventral cord

850 acetylcholine motor neuron promoter (*acr-2p*, transgene *yakEx47*), and interneuron promoter

851 (*nmr-1p*, transgene *yakSi32*). Shown is the number of squares single animals covered in ~20 h.

852 (****, P<0.0001. ns, P>0.05. One way ANOVA followed by a Bonferroni test. Error bars = SEM;
853 n = 15).
854 (B) Expression of *grk-2* cDNA under either of two ciliated sensory neuron promoters (*xbx-1p*,
855 transgene *yakEx71* and *osm-6p*, transgene *yakEx53*) rescues the exploration defect of *grk-*
856 *2(gk268)* mutant animals in the presence of food. (****, P<0.001. ns, P>0.05. One way ANOVA
857 followed by a Bonferroni test. Error bars = SEM; n = 15-20).
858 (C) Expression of *grk-2* cDNA under a ciliated sensory neuron promoter (*xbx-1p::grk-2*,
859 transgene *yakEx71*) rescues the dispersal defect of *grk-2(gk268)* in the absence of food. (****,
860 P<0.0001. ***, P<0.001. ns, P>0.05. One way ANOVA followed by a Bonferroni test. Error bars
861 = SEM; n = 25-31).
862 (D) Expression of *grk-2* cDNA under the *odr-3* promoter (expression in AWA, AWB, AWC, ASH,
863 and ADF neurons; *odr-3p::grk-2*, transgene *yakEx189*) partially rescues the exploration defect
864 of *grk-2(gk268)*. (****, P<0.0001. ***, P<0.001. One way ANOVA followed by a Bonferroni test.
865 Error bars = SEM; n = 12-34).
866 (E) Expression of *grk-2* cDNA under the *sra-6* promoter (expression in ASH and ASI neurons;
867 *sra-6p::grk-2*, transgene *yakEx191*) or under the combined control of the *odr-10* (AWA
868 neurons), *str-1* (AWB neurons) and *str-2* (AWC ON neuron) promoters (*str-1p, str-2p, odr-*
869 *10p::grk-2*, transgene *yakEx194*) partially rescues the exploration defect of *grk-2(gk268)*.
870 (F) Expression of *grk-2* cDNA under the *odr-10p* (AWA), *str-1p* (AWB), or *str-2p* (AWC ON)
871 promoters (transgenes *pekEx267, pekEx265* and *pekEx266,* respectively) partially rescues the
872 *grk-2* exploration defect. (****, P<0.0001. **, P<0.01. *, P<0.05. One way ANOVA followed by a
873 Bonferroni test. Error bars = SEM; n = 17-34).
874 (G) *grk-2* is expressed in many neurons in the head of the worm including *odr-3*- expressing
875 neurons. Representative images of the z-stack projections of the head of an animal co-
876 expressing tagRFP fused to GRK-2 ORF driven by the *grk-2* promoter (*grk-2*::tagRFP,
877 transgene *yakIs19*) and NLS-tagged mNeon driven by the *odr-3* promoter (*odr-3p*::mNeon::NLS;

878 transgene *yakEx204*). Arrows indicate *grk-2*::tagRFP-expressing cells that also express *odr-*
879 *3p*::mNeon::NLS. Scale bar: 10 μm.
880 (H) Expression of *grk-2* cDNA under the *gcy-8* promoter (expression in AFD neurons; *gcy-*
881 *8p::grk-2*, transgene *yakEx202*) fails to rescue the exploration defect of *grk-2(gk268)*.
882 (ns, P>0.05. One way ANOVA followed by a Bonferroni test. Error bars = SEM; n = 20-30).
883 (I) Expression of *grk-2* cDNA under the *dat-1* promoter (expression in dopaminergic neurons;
884 *dat-1p::grk-2*, transgene *yakEx259*) fails to rescue the exploration defect of *grk-2(gk268)*. (ns,
885 P>0.05. Student's t-test. Error bars = SEM; n = 30-32).
886 (J) Expression of *grk-2* cDNA under the heat shock promoter *hsp-16.41* (*hsp-16.41p::grk-2*,
887 transgene *yakEx253*) in adult *grk-2(gk268)* partially but significantly rescues their exploration
888 defect. (****, P<0.0001. Student's t-test. Error bars = SEM; n = 26-32).
889
890 **Fig 3. Mutants in cilia-related genes have exploration defects.**
891 (A) The *che-2(e1033)* mutant has an exploration defect like *grk-2(gk268)* that is not enhanced
892 by *grk-2*. Shown is the number of squares single animals covered in ~20 h. (****, P<0.0001. ns,
893 P>0.05. One way ANOVA followed by a Bonferroni test. Error bars = SEM; n = 15).
894 (B) The *daf-10(e1387)* mutant has an exploration defect like *grk-2(gk268)* that is not enhanced
895 by *grk-2*. Shown is the number of squares single animals covered in ~20 h. (****, P<0.0001. ns,
896 P>0.05. One way ANOVA followed by a Bonferroni test. Error bars = SEM; n = 20-25).
897 (C) The *che-2(e1033)* and *daf-10(e1387)* mutants have a dispersal defect independently of food
898 that is not enhanced by *grk-2(gk268).* Shown is the distance (cm) animals traveled from the
899 center of the plate without food in 20 min. (****, P<0.0001. One way ANOVA followed by a
900 Bonferroni test. Error bars = SEM; n = 30-40).
901 (D) Most chemosensory and osmosensory-defective mutants that possess strong or weak
902 cilium-structure defects based on a dye-filling assay ([46]; shown in blue and green,
903 respectively) have exploration defects. Chemosensory-defective mutants *odr-1, odr-3, odr-8,*

904 *odr-10, tax-2,* and *tax-4*; osmosensory-defective mutants *osm-7* and *osm-10;* and
905 thermosensory-defective mutant *ttx-1(p767),* also have exploration defects. In contrast,
906 chemosensory mutants *che-1, che-6, che-7, odr-2, odr-4, odr-5, odr-7,* osmosensory mutants
907 *osm-9* and *osm-11*, oxygen-sensing mutant *gcy-35,* and mechanosensory-defective mutants
908 *mec-3, mec-4,* and *glr-1* do not have exploration defects. The canonical null allele *ocr-2(ak47)*
909 (strain VM396; indicated with an asterisk) showed a significant exploration defect that was not
910 observed with the presumably null allele *ocr-2(ok1711)*. Outcrossed strain BJH2763 *ocr-2(ak47)*
911 did not show a similar exploration defect, suggesting that the *ocr-2(ak47)* mutation per se does
912 not cause exploration defects (Fig S3A; see text for details). Shown is the number of squares
913 (out of 50) single animals covered in ~20 h, normalized to WT. (***, P<0.001. **, P<0.01. *,
914 P<0.05. ns, P>0.05. One way ANOVA followed by a Bonferroni test. Error bars = SEM; n = 10-
915 35).
916
917 **Fig 4. *egl-4* suppresses the exploration defect, movement quiescence, and reduced**
918 **activity of *grk-2* mutant animals.**
919 (A), (B) The *egl-4(n479)* mutation partially suppresses the exploration defect of *grk-2(gk268)*
920 mutant as assayed on 6 cm (A) and 10 cm (B) plates. Shown is the number of squares (out of
921 50, (A) or 150, (B)) single animals covered in ~20 h. Please note that *egl-4* mutant animals
922 explore more than wild type animals as assayed on 10 cm plates. (****, P<0.0001. ***, P<0.001.
923 ns, P>0.05. One way ANOVA followed by a Bonferroni test. Error bars = SEM; n = 16-20).
924 (C) Expression of *egl-4* cDNA in ciliated sensory neurons under the *osm-6* promoter reverses
925 the *egl-4* suppression of the exploration defect of *grk-2* mutant (*osm-6p::egl-4*, transgene
926 *yakEx221*). Shown is the number of squares single animals covered in ~20 h (****, P<0.0001.
927 ns, P>0.05. Student's t-test. Error bars = SEM; n = 31-33).
928 (D) *grk-2(gk268)* mutant animals show enhanced movement quiescence, and the *egl-4(n479)*
929 mutation suppresses this phenotype. The graph shows the average minutes animals spent in

930 quiescence per hour in the WorMotel. Quiescence is the time when zero worm pixels moved
931 between two frames separated by 10 sec (See Methods). One WT animal was considered an
932 outlier and was not included in the graph since its values were more than 3 standard deviations
933 from the mean.
934 (E) The graph shows the total minutes individual animals spent in quiescence in 8 h in the
935 WorMotel. (****, P<0.0001. ns, P>0.05. One way ANOVA. Error bars = SEM; n = 11-12).
936 (F) *grk-2(gk268)* mutant animals show reduced activity, and the *egl-4(n479)* mutation partially
937 suppresses this phenotype. The graph shows the activity in pixels of individual animals in 8 h in
938 the WorMotel. Activity is the number of pixels moved between frames separated by 10 sec.
939 (****, P<0.0001. One way ANOVA. Error bars = SEM; n = 11-12).
940
941 **Fig 5. *aptf-1* partially suppresses the exploration defect, movement quiescence, and**
942 **reduced activity of *grk-2*.**
943 (A) The *aptf-1(gk794)* mutation partially suppresses the exploration defect of *grk-2(gk268)*
944 mutant. Shown is the number of squares single animals covered in ~20 h. (****, P<0.0001. ns,
945 P>0.05. One way ANOVA followed by a Bonferroni test. Error bars = SEM; n = 20-21).
946 (B) *grk-2(gk268)* mutant animals show enhanced movement quiescence, and the *aptf-1(gk794)*
947 mutation partially suppresses this phenotype. The graph shows the average minutes animals
948 spent in quiescence per hour in the WorMotel. Quiescence is the time when zero pixels moved
949 between two frames separated by 10 sec (See Methods).
950 (C) *grk-2(gk268)* mutant animals show enhanced movement quiescence, and the *aptf-1(gk794)*
951 mutation partially suppresses this phenotype. The graph shows the total minutes individual
952 animals spent in quiescence in 8 h in the WorMotel. (****, P<0.0001. ns, P>0.05. One way
953 ANOVA. Error bars = SEM; n = 10-12).

954 (D) *grk-2(gk268)* mutant animals show reduced activity, and the *aptf-1(gk794)* mutation partially
955 suppresses this phenotype. The graph shows the activity in pixels of individual animals in 8 h in
956 the WorMotel. Activity is the number of pixels moved between frames separated by 10 sec.
957 (****, P<0.05. **, P<0.01. One way ANOVA. Error bars = SEM; n = 10-12).
958
959 **Fig 6. *npr-1* suppresses the exploration defect of *grk-2* mutant animals.**
960 (A) The *npr-1(ky13)* mutation suppresses the exploration defect of *grk-2(gk268)* mutants as
961 assayed on 6 cm plates. Shown is the number of squares (out of 50) single animals covered in
962 ~20 h. (****, P<0.0001. *, P<0.05. ns, P>0.05. One way ANOVA followed by a Bonferroni test.
963 Error bars = SEM; n = 18-38).
964 (B) The *npr-1(ky13)* mutation suppresses the exploration defect of *grk-2(gk268)* mutant as
965 assayed on 10 cm plates. Shown is the number of squares (out of 150) single animals covered
966 in ~20 h. (****, P<0.0001. **, P<0.01. ns, P>0.05. One way ANOVA followed by a Bonferroni
967 test. Error bars = SEM; n = 13).
968 (C) The *npr-1(ky13)* mutation suppresses the dispersal defect of *grk-2(gk268)* in the absence of
969 food. (***, P<0.001. **, P<0.01. *, P<0.05. ns, P>0.05. One way ANOVA followed by a
970 Bonferroni test. Error bars = SEM; n = 17-19).
971 (D) The *flp-18(db99)* mutation partially but significantly suppresses the exploration defect of *grk-*
972 *2(gk268)*. (****, P<0.0001. ns, P>0.05. One way ANOVA followed by a Bonferroni test. Error
973 bars = SEM; n = 18-29).
974 (E) The *flp-21(ok889)* mutation does not suppress the exploration defect of *grk-2(gk268)*. (****,
975 P<0.0001. **, P<0.01. ns, P>0.05. One way ANOVA followed by a Bonferroni test. Error bars =
976 SEM; n = 12-26).
977 (F) Expression of *ncs-1p::nCre* and *flp-21p*::LoxStopLox::NPR-1 (expression in RMG neurons
978 ((54); *RMGp::npr-1*, transgene *yakEx206*) reverses the *npr-1* suppression of the exploration
979 defect of *grk-2(gk268)* mutant. Expression of *npr-1* cDNA under the *sra-6* promoter (expression

980 in ASH and ASI neurons; *sra-6p::npr-1*, transgene *yakEx209*) fails to reverse the *npr-1*
981 suppression of the exploration defect of *grk-2(gk268)* (****, P<0.0001. ns, P>0.05. One way
982 ANOVA followed by a Bonferroni test. Error bars = SEM; n = 16-23).
983
984 **Fig 7. *flp-1* significantly suppresses the exploration defect of *grk-2*.**
985 (A) *grk-2(gk268)* mutant animals have an exploration defect and *flp-1(ok2811)* significantly
986 suppresses this defect. Shown is the number of squares (out of 50) single animals covered in
987 ~20 h. (****, P<0.0001. One way ANOVA followed by a Bonferroni test. Error bars = SEM; n =
988 20-25).
989 (B) *flp-1* and *flp-18* act in the same pathway to regulate exploration. *flp-1(ok2811)* and *flp-*
990 *18(db99)* partially suppress the exploration defect of *grk-2(gk268)* mutant and the *grk-2(gk268);*
991 *flp-1(ok2811); flp-18(db99)* triple mutant behaves like the *grk-2(gk268); flp-1(ok2811)* double
992 mutant. (****, P<0.0001. ***, P<0.001. ns, P>0.05. One way ANOVA followed by a Bonferroni
993 test. Error bars = SEM; n = 14-28).
994 (C) Expression of *flp-1* under its own promoter (*flp-1p::flp-1*, transgene *yakEx231*) or under the
995 *twk-47* promoter (expression in AVK neurons; *twk-47p::flp-1*, transgene *yakEx216),* reverses the
996 *flp-1* suppression of the exploration defect of *grk-2(gk268)* mutant. (****, P<0.0001. Student's t-
997 test. Error bars = SEM; n = 23-30).
998 (D) *npr-1(ky13)* suppresses the dispersal defect of *grk-2(gk268)* mutant and the *grk-2(gk268);*
999 *flp-1(ok2811); npr-1(ky13)* triple mutant behaves like the *grk-2(gk268); npr-1(ky13)* double
1000 mutant. Shown is the distance (cm) animals traveled from the center of the plate in the presence
1001 of food in 1 h. (ns, P>0.05. One way ANOVA followed by a Bonferroni test. Error bars = SEM; n
1002 = 51-67).
1003 (E) *npr-1(ky13)* suppresses the exploration defect of *grk-2(gk268)* mutant and the *grk-2(gk268);*
1004 *flp-1(ok2811); npr-1(ky13)* triple mutant behaves like the *grk-2(gk268); npr-1(ky13)* double

1005 mutant. Shown is the number of squares (out of 50) single animals covered in ~20 h (ns,
1006 P>0.05. One way ANOVA followed by a Bonferroni test. Error bars = SEM; n = 15-28).
1007 (F) *frpr-7(gk463846)* partially but significantly suppresses the exploration defect of *grk-2(gk268)*
1008 mutant. *npr-6(tm1497)* has no effect on *grk-2(gk268)* exploration. (***, P<0.001. ns, P>0.05.
1009 One way ANOVA followed by a Bonferroni test. Error bars = SEM; n = 23-39).

1010 **Fig 8. *grk-2* mutant animals expressing FLP-1::mCherry show increased fluorescence in**
1011 **their coelomocytes.**
1012 (A) (Up) Schematic diagram of the coelomocyte uptake assay used to quantify FLP-1 secretion
1013 from AVK interneurons. (Down) Representative images of coelomocytes of *flp-1(ok2811)* and
1014 *grk-2(gk268); flp-1(ok2811)* mutant animals expressing a rescuing construct of FLP-1::mCherry
1015 (FLP-1::mCherry; transgene *yakEx256*). Scale bars = 10 μm.
1016 (B) mCherry fluorescence intensity of coelomocytes of *flp-1(ok2811)* and *grk-2(gk268); flp-*
1017 *1(ok2811)* mutant animals expressing FLP-1::mCherry and a coelomocyte marker *unc-*
1018 *122*::GFP. (FLP-1::mCherry; transgene *yakEx256).* (**, P<0.01. Student's t-test. Error bars =
1019 SEM; n = 57-59).
1020 (C) GFP fluorescence intensity of coelomocytes of *flp-1(ok2811)* and *grk-2(gk268); flp-*
1021 *1(ok2811)* mutant animals expressing FLP-1::mCherry and a coelomocyte marker *unc-*
1022 *122*::GFP (*unc-122::GFP*; transgene *yakEx256*). (ns, P>0.05. Student's t-test. Error bars =
1023 SEM; n = 29-30).
1024 (D) Overexpression of FLP-1 reduces the exploration behavior of wild type animals. Shown is
1025 the number of squares covered in ~20 h by single wild type animals, *flp-1* mutant expressing
1026 low levels of FLP-1::mCherry (transgene *yakEx256;* 5 ng/ul injected), and wild type animals
1027 overexpressing FLP-1 (transgene *yakEx261;* 60 ng/ul injected). (****, P<0.0001. ***, P<0.001.
1028 One way ANOVA followed by a Bonferroni test. Error bars = SEM; n = 21-47).
1029

1030 **Fig 9. Model for GRK-2 modulation of locomotion behaviors in *C. elegans.***

1031 GRK-2 positively regulates (A) crawling and swimming by acting in premotor interneurons in a
1032 manner that depends on the D2-like dopamine receptor DOP-3 [27,28] and (B) exploration by
1033 acting in ciliated neurons in an opposite way from EGL-4. We propose a model in which GRK-2
1034 acts in multiple ciliated sensory neurons to positively control sensory perception and (1) inhibit
1035 the activity of the EGL-4 kinase in ciliated neurons, (2) negatively regulate the neuropeptide
1036 receptor NPR-1 in RMG interneurons, and (3) negatively control the levels of FLP-1 secretion
1037 from AVK interneurons. Since the ciliated neurons and AVK interneurons do not have direct
1038 connections, we propose that GRK-2 controls FLP-1 secretion from AVK interneurons in a non-
1039 cell autonomous way through a neuromodulatory pathway. Proteins that positively regulate
1040 crawling, swimming, or exploration are shown in green and proteins that negatively regulate
1041 crawling, swimming, or exploration are shown in red. Dashed lines show indirect interactions.
1042

Figure 1

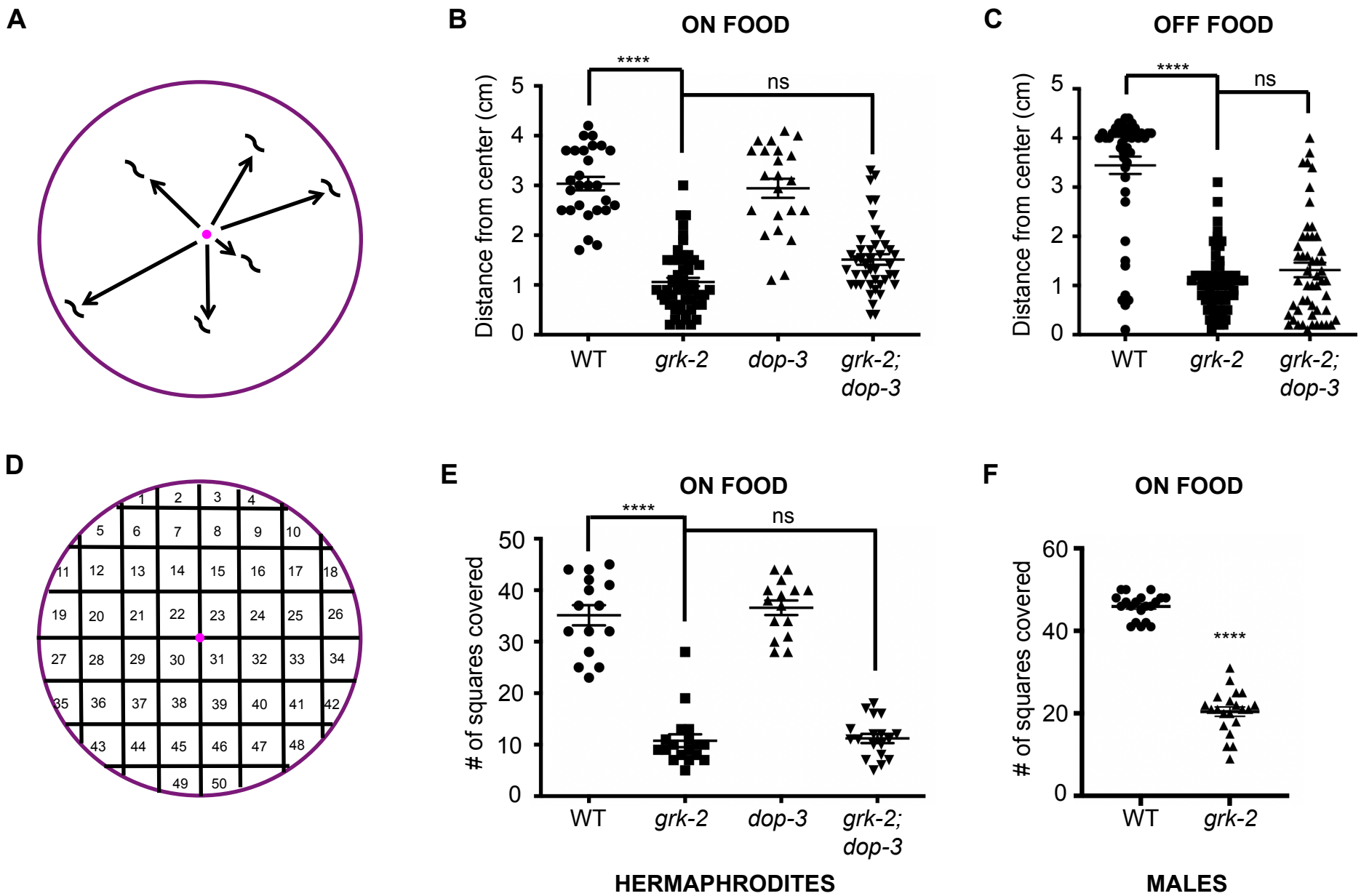
A
B
ON FOOD
Distance from center (cm)
****
ns
WT
grk-2
dop-3
grk-2; dop-3
C
OFF FOOD
Distance from center (cm)
****
ns
WT
grk-2
grk-2; dop-3
D
1 2 3 4 5 6 7 8 9 10 11 12 13 14 15 16 17 18 19 20 21 22 23 24 25 26 27 28 29 30 31 32 33 34 35 36 37 38 39 40 41 42 43 44 45 46 47 48 49 50
E
ON FOOD
# of squares covered
****
ns
WT
grk-2
dop-3
grk-2; dop-3
HERMAPHRODITES
F
ON FOOD
# of squares covered
****
WT
grk-2
MALES

Figure 2

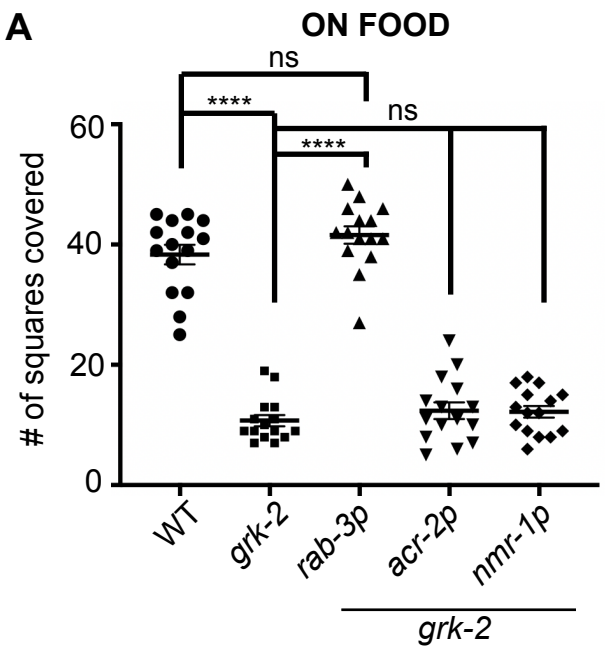

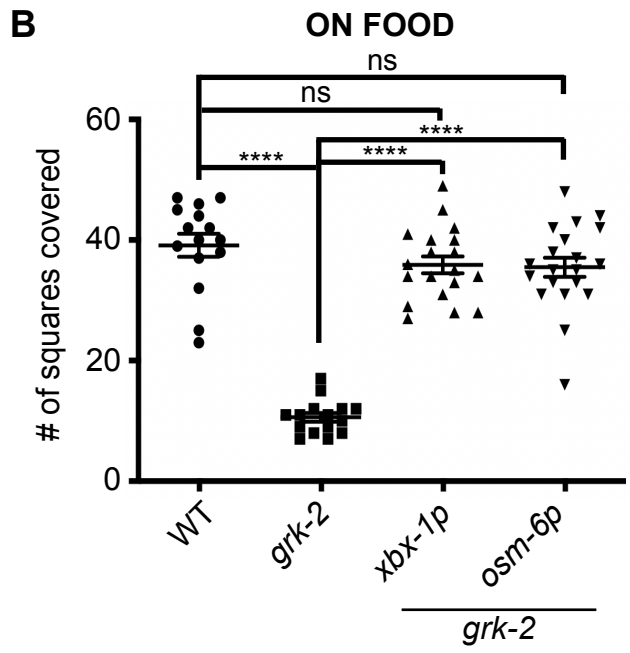

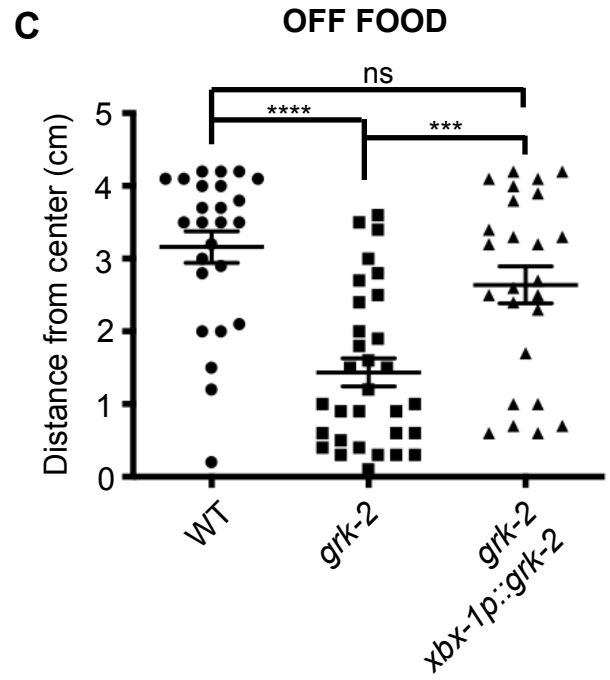

rab-3: **All neurons**
acr-2: **Ventral Cord motor neurons**
nmr-1: **Command interneurons**

xbx-1, osm-6: **Ciliated neurons**

xbx-1: **Ciliated neurons**

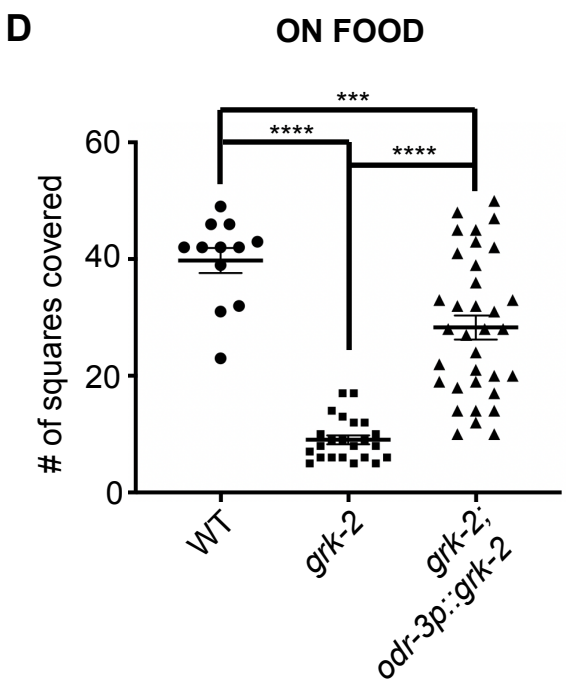

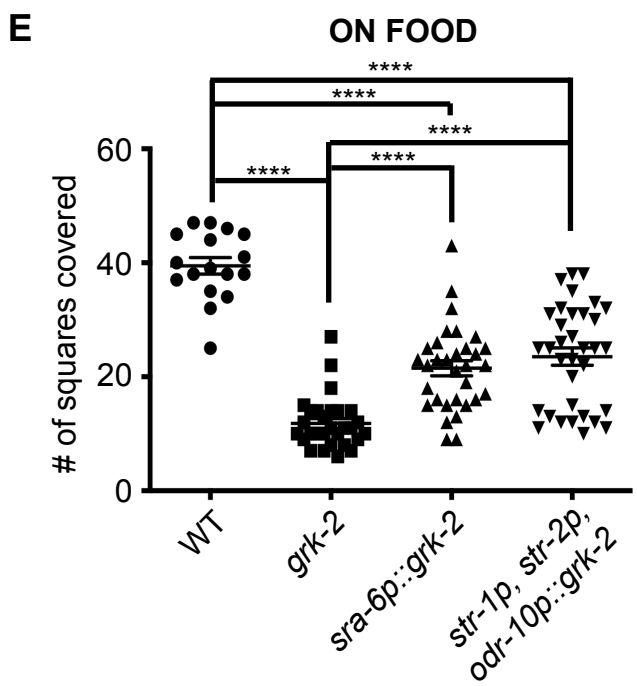

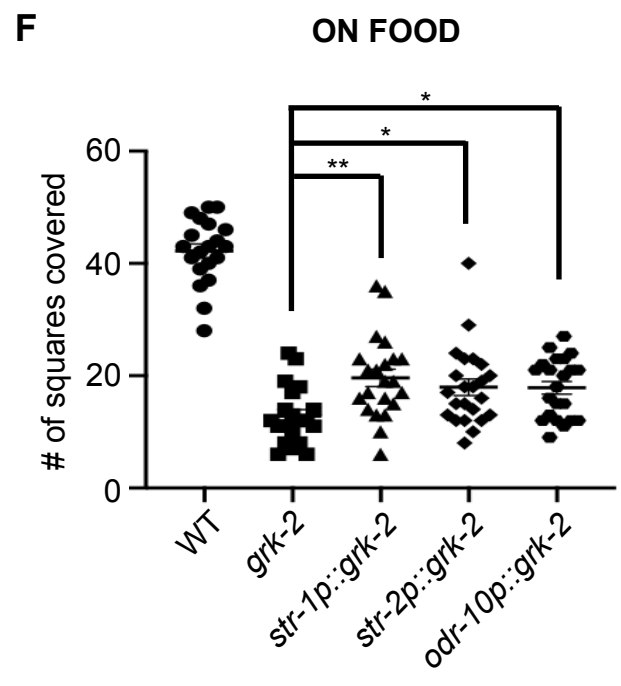

odr-3: **AWA, AWB, AWC, ASH, ADF**

sra-6: **ASH, ASI**
odr-10: **AWA**
str-1: **AWB**
str-2: **AWC ON**

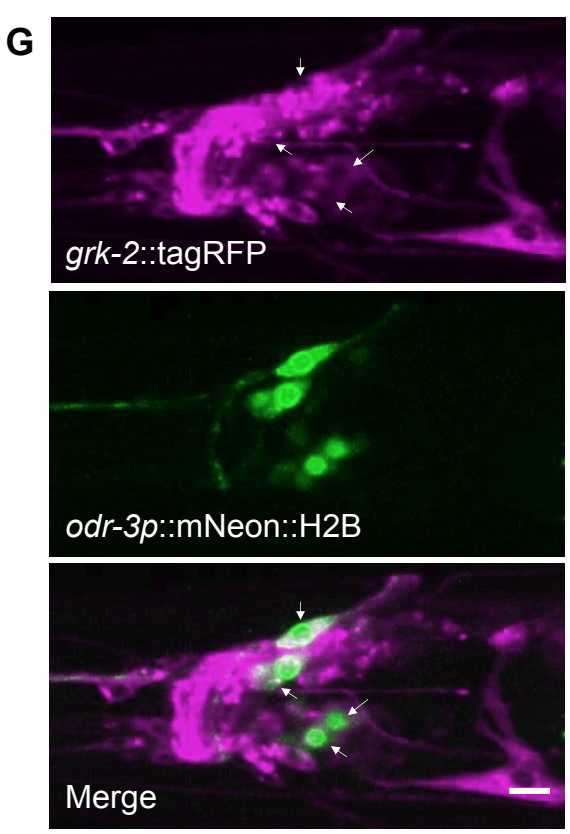

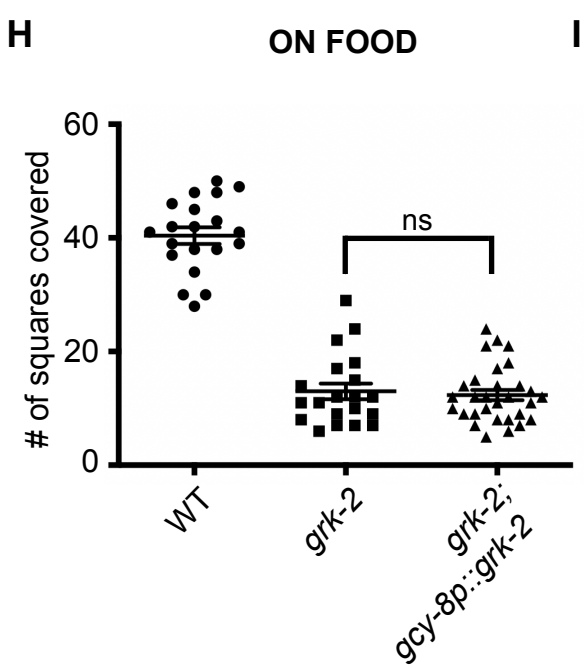

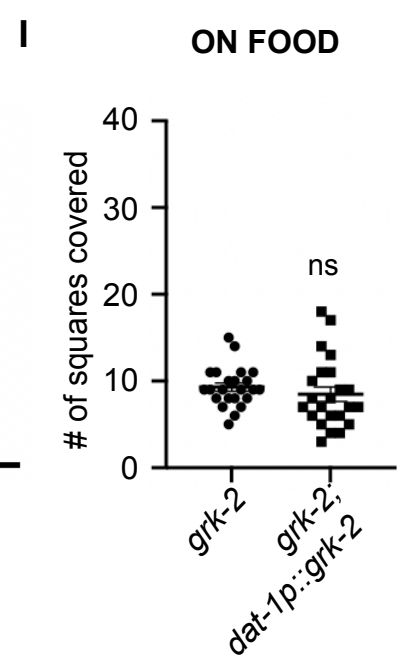

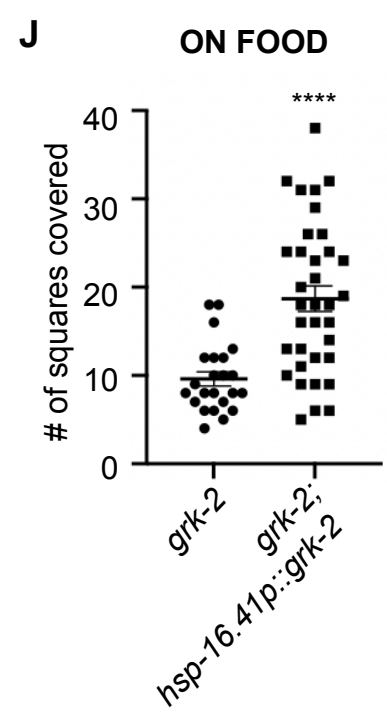

gcy-8: **AFD**

dat-1: **dopamine neurons**

Figure 3

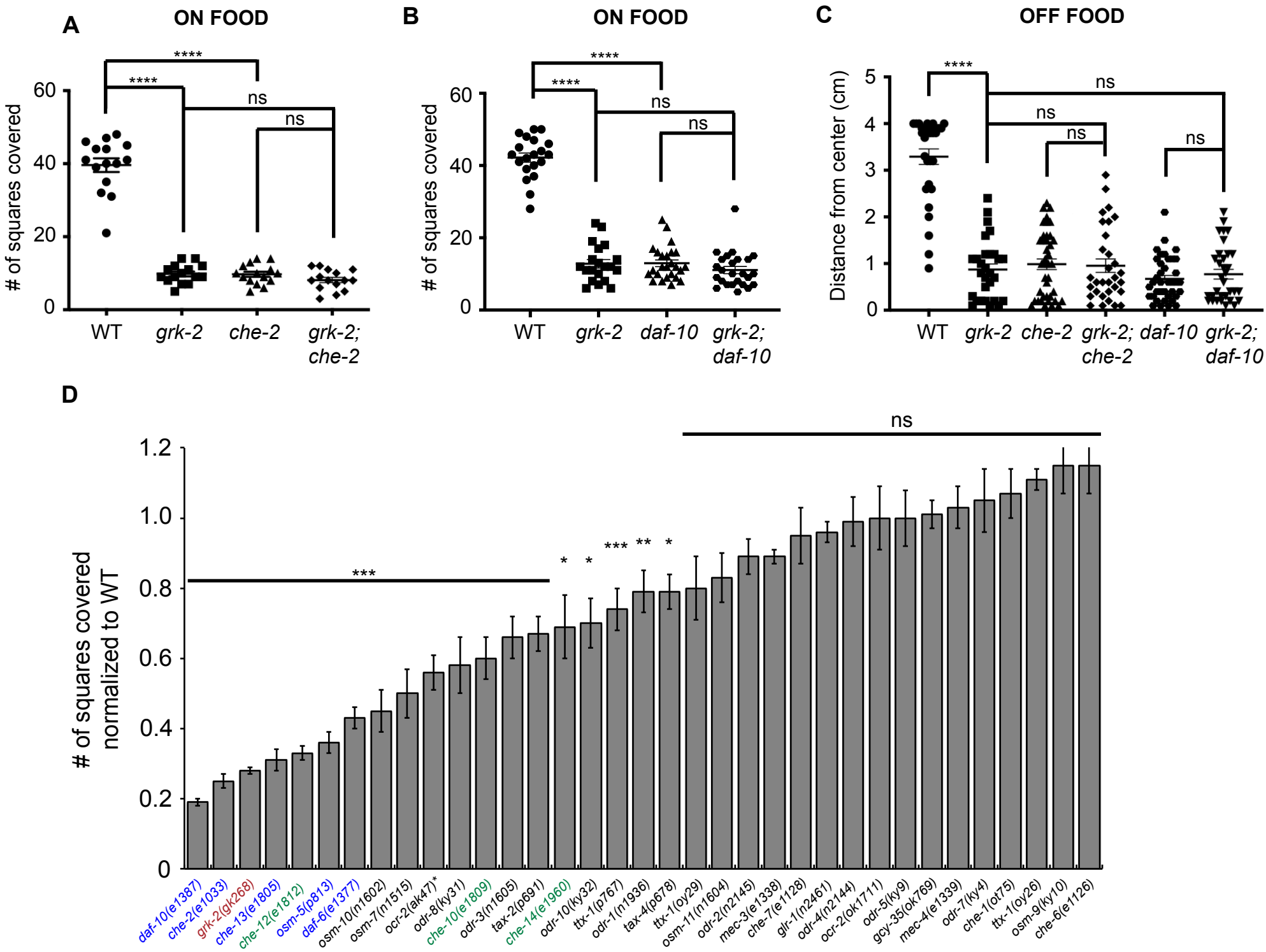
A
ON FOOD
# of squares covered
****
****
ns
ns
WT
grk-2
che-2
grk-2; che-2
B
ON FOOD
# of squares covered
****
****
ns
ns
WT
grk-2
daf-10
grk-2; daf-10
C
OFF FOOD
Distance from center (cm)
****
ns
ns
ns
ns
WT
grk-2
che-2
grk-2; che-2
daf-10
grk-2; daf-10
D
# of squares covered normalized to WT
ns
***
daf-10(e1387)
che-2(e1033)
grk-2(gk268)
che-13(e1805)
che-12(e1812)
osm-5(p813)
daf-6(e1377)
osm-10(n1602)
osm-7(n1515)
ocr-2(ak47)*
odr-8(ky31)
che-10(e1809)
odr-3(n1605)
tax-2(p691)
che-14(e1960)
odr-10(ky32)
ttx-1(p767)
odr-1(n1936)
tax-4(p678)
ttx-1(oy29)
osm-11(n1604)
odr-2(n2145)
mec-3(e1338)
che-7(e1128)
glr-1(n2461)
odr-4(n2144)
ocr-2(ok1711)
odr-5(ky9)
gcy-35(ok769)
mec-4(e1339)
odr-7(ky4)
che-1(ot75)
ttx-1(oy26)
osm-9(ky10)
che-6(e1126)

Figure 4

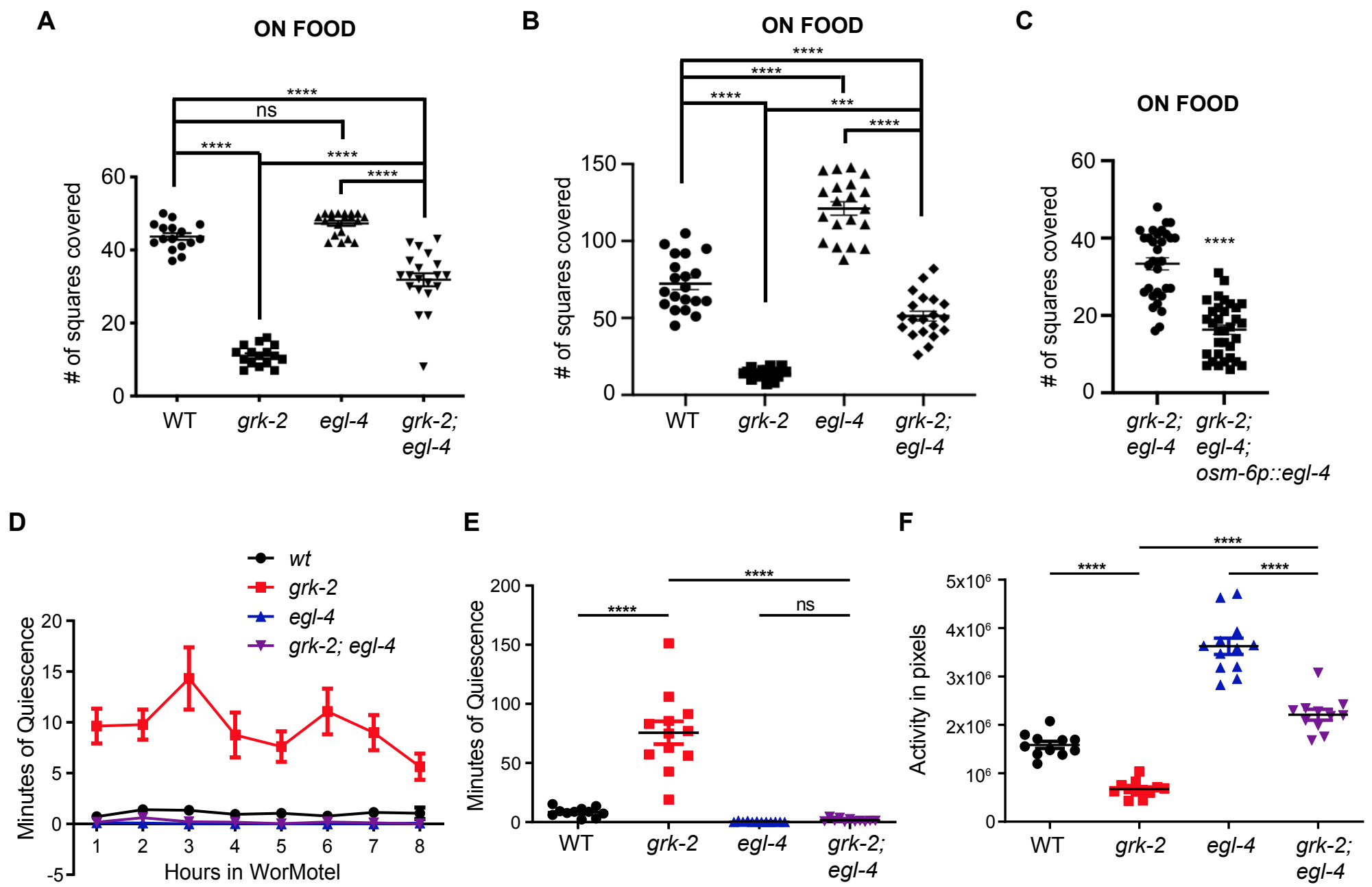
A
ON FOOD
# of squares covered
WT
grk-2
egl-4
grk-2; egl-4
ns
B
ON FOOD
# of squares covered
C
ON FOOD
# of squares covered
grk-2; egl-4
grk-2; egl-4; osm-6p::egl-4
D
wt
grk-2
egl-4
grk-2; egl-4
Minutes of Quiescence
Hours in WorMotel
E
Minutes of Quiescence
F
Activity in pixels

Figure 5

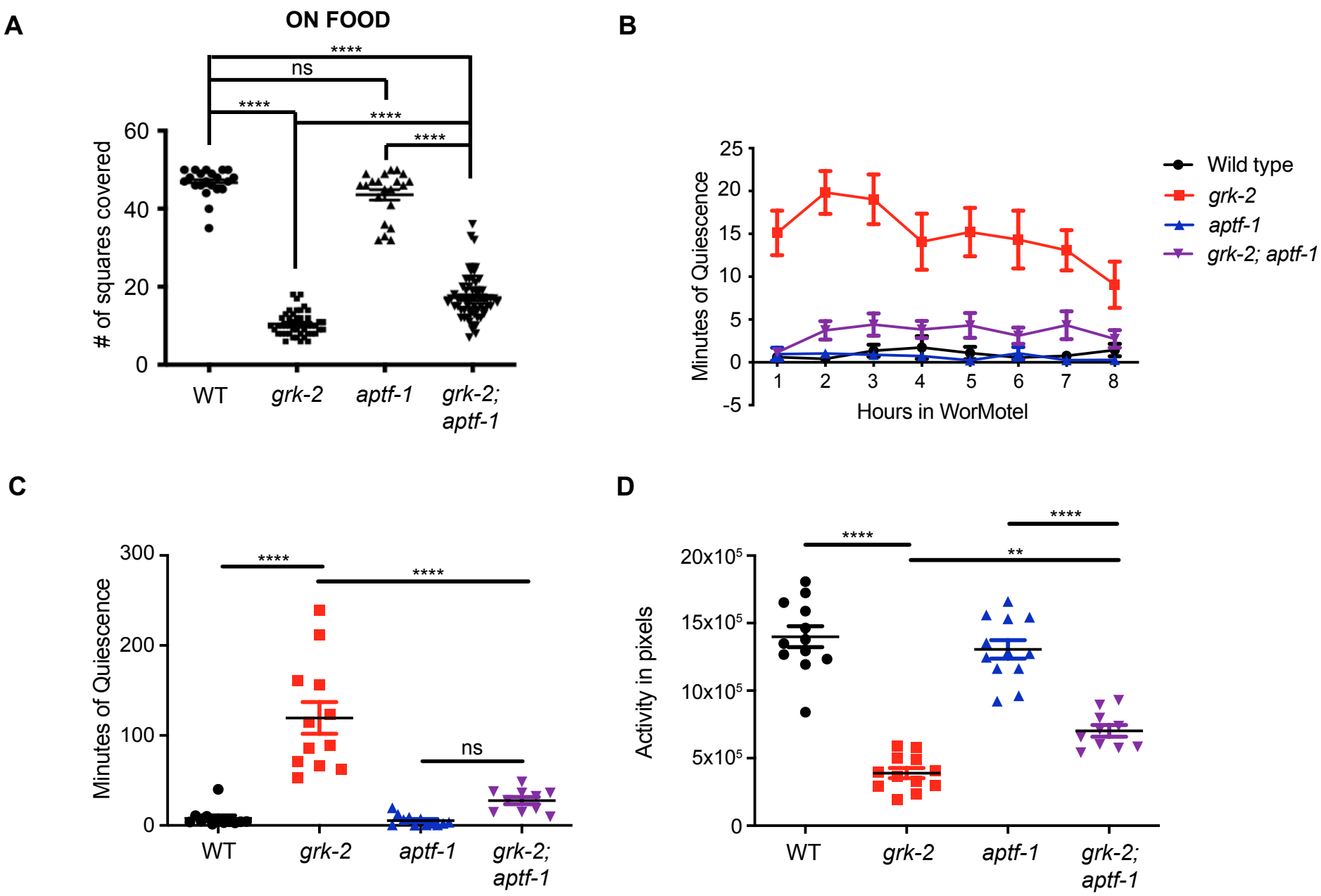
A
ON FOOD
****
ns
****
****
****
# of squares covered
60
40
20
0
WT
grk-2
aptf-1
grk-2; aptf-1
B
Minutes of Quiescence
25
20
15
10
5
0
-5
1
2
3
4
5
6
7
8
Hours in WorMotel
Wild type
grk-2
aptf-1
grk-2; aptf-1
C
Minutes of Quiescence
300
200
100
0
****
****
ns
WT
grk-2
aptf-1
grk-2; aptf-1
D
Activity in pixels
20x10^5
15x10^5
10x10^5
5x10^5
0
****
****
**
WT
grk-2
aptf-1
grk-2; aptf-1

Figure 6

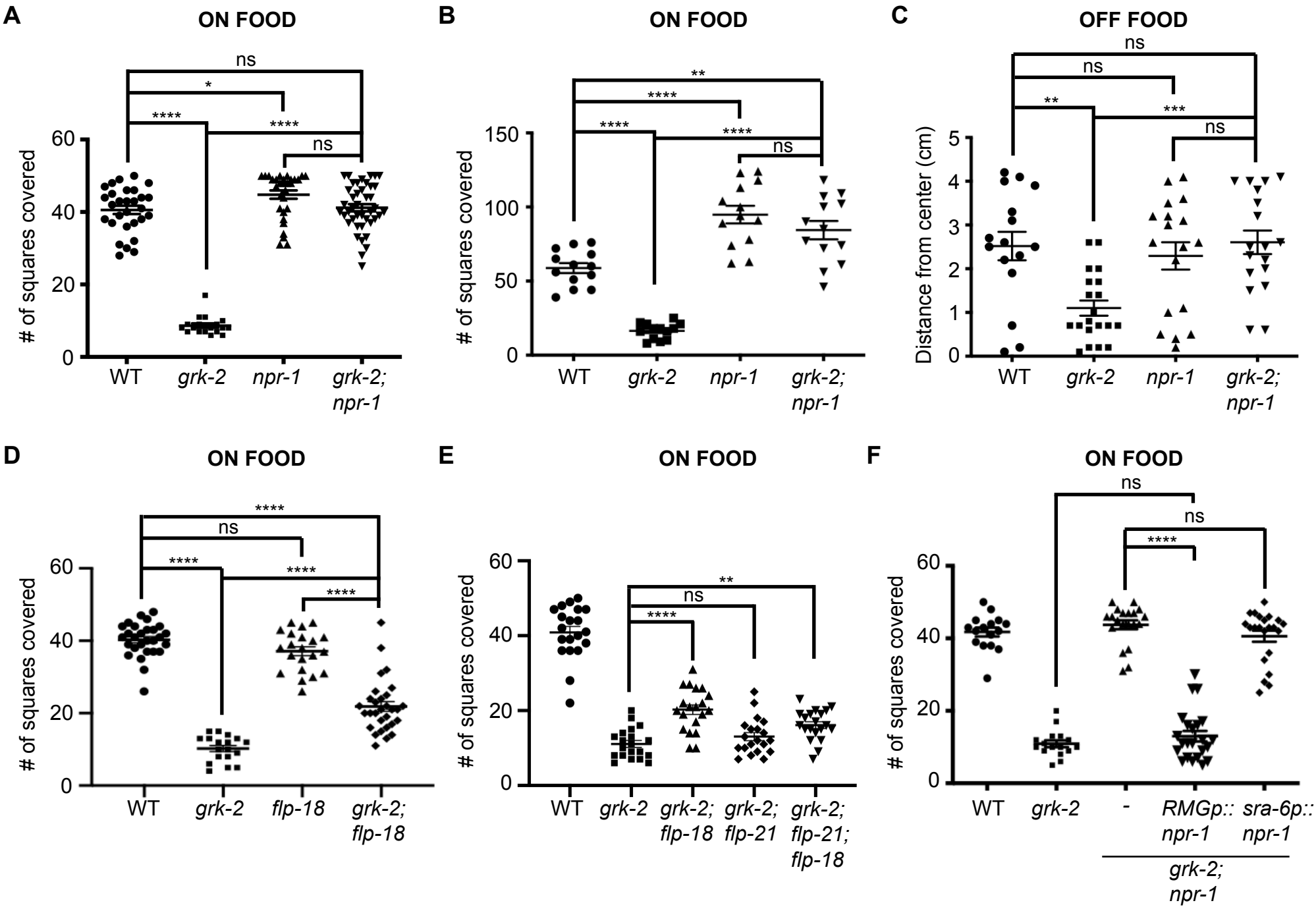
A
ON FOOD
# of squares covered
ns
*
****
****
ns
WT
grk-2
npr-1
grk-2; npr-1
B
ON FOOD
# of squares covered
**
****
****
****
ns
WT
grk-2
npr-1
grk-2; npr-1
C
OFF FOOD
Distance from center (cm)
ns
ns
**
***
ns
WT
grk-2
npr-1
grk-2; npr-1
D
ON FOOD
# of squares covered
****
ns
****
****
****
WT
grk-2
flp-18
grk-2; flp-18
E
ON FOOD
# of squares covered
**
ns
****
WT
grk-2
grk-2; flp-18
grk-2; flp-21
grk-2; flp-21; flp-18
F
ON FOOD
# of squares covered
ns
ns
****
WT
grk-2
-
RMGp:: npr-1
sra-6p:: npr-1
grk-2; npr-1

Figure 7

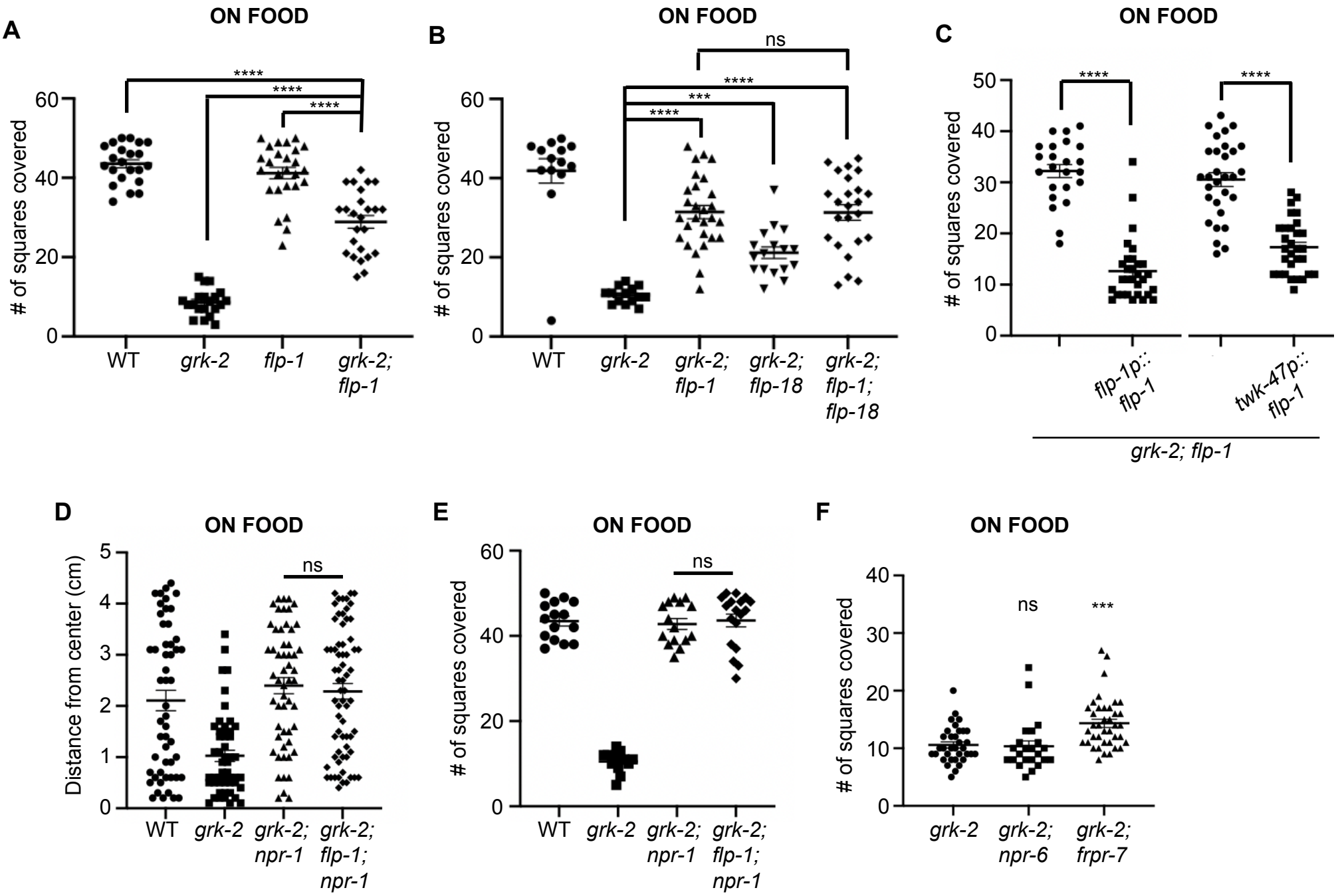
A
ON FOOD
# of squares covered
****
****
****
WT
grk-2
flp-1
grk-2; flp-1
B
ON FOOD
# of squares covered
ns
****
***
****
WT
grk-2
grk-2; flp-1
grk-2; flp-18
grk-2; flp-1; flp-18
C
ON FOOD
# of squares covered
****
****
flp-1p::flp-1
twk-47p::flp-1
grk-2; flp-1
D
ON FOOD
Distance from center (cm)
ns
WT
grk-2
grk-2; npr-1
grk-2; flp-1; npr-1
E
ON FOOD
# of squares covered
ns
WT
grk-2
grk-2; npr-1
grk-2; flp-1; npr-1
F
ON FOOD
# of squares covered
ns
***
grk-2
grk-2; npr-6
grk-2; frpr-7

Figure 8

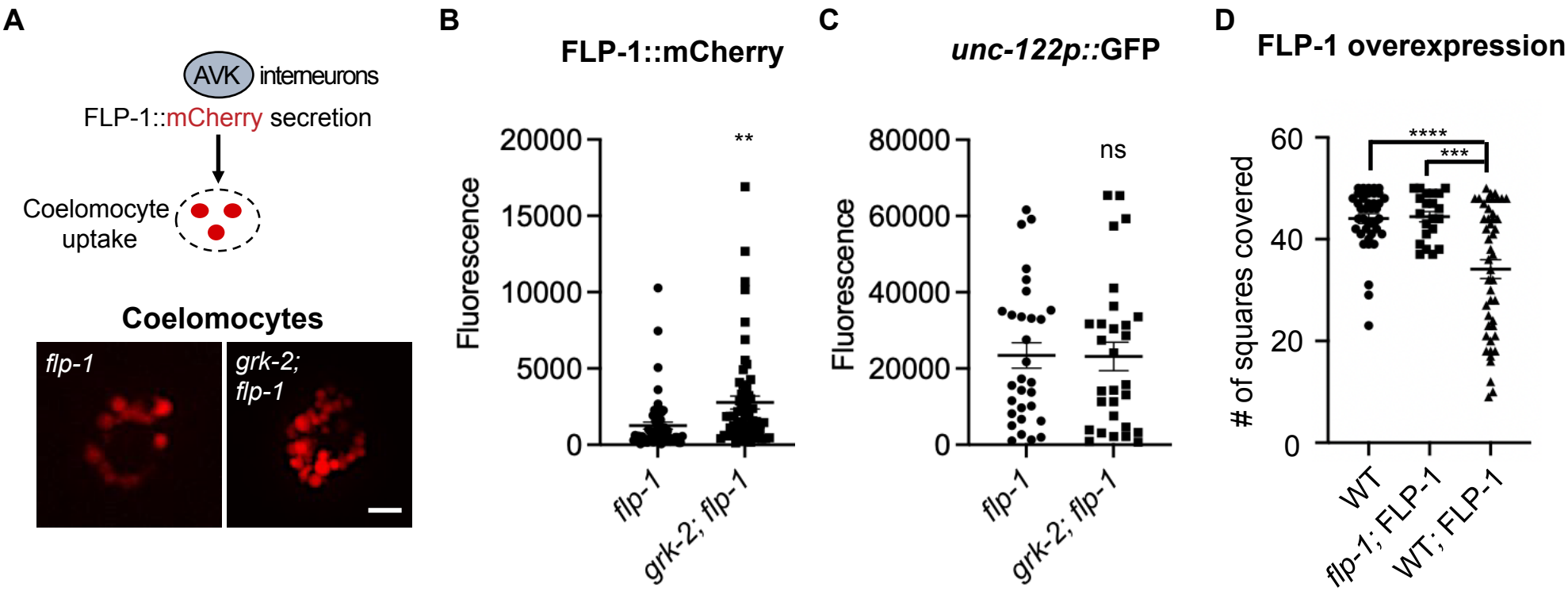
A
AVK interneurons
FLP-1::mCherry secretion
Coelomocyte uptake
Coelomocytes
flp-1
grk-2; flp-1
B
FLP-1::mCherry
Fluorescence
20000
15000
10000
5000
0
**
flp-1
grk-2; flp-1
C
unc-122p::GFP
Fluorescence
80000
60000
40000
20000
0
ns
flp-1
grk-2; flp-1
D
FLP-1 overexpression
# of squares covered
60
40
20
0
****
***
WT
flp-1; FLP-1
WT; FLP-1

Figure 9

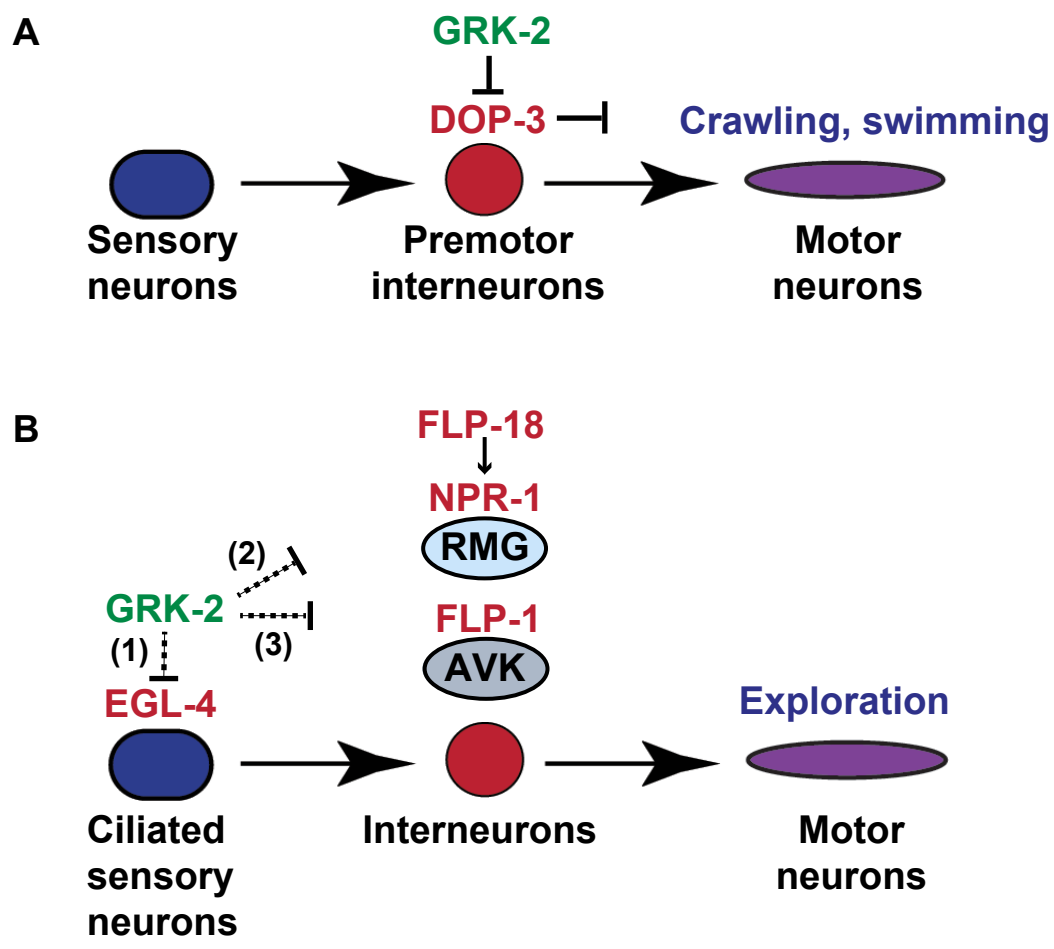
A
GRK-2
DOP-3
Crawling, swimming
Sensory neurons
Premotor interneurons
Motor neurons
B
FLP-18
NPR-1
RMG
(2)
GRK-2
(1)
(3)
FLP-1
AVK
EGL-4
Exploration
Ciliated sensory neurons
Interneurons
Motor neurons